

# **A BIOMATHEMATICAL MODEL ON THE RUPTURE OF INTRACRANIAL ANEURYSMS**

by

**Yixiang Feng**

December 19, 2002

A thesis submitted to the  
Faculty of the Graduate School of  
State University of New York at Buffalo  
in partial fulfillment of the requirements for the degree of

**Master of Science**

Department of Mechanical and Aerospace Engineering

# TABLE OF CONTENTS

<b>ACKNOWLEDGMENTS</b> .....	<b>V</b>
<b>NOMENCLATURE</b> .....	<b>VI</b>
<b>LIST OF FIGURES</b> .....	<b>VII</b>
<b>ABSTRACT</b> .....	<b>X</b>
<b>CHAPTER 1 INTRODUCTION</b> .....	<b>1</b>
1.1 INTRACRANIAL ANEURYSMS .....	1
1.2 MATHEMATICAL MODELING .....	2
1.3 OBJECTIVES AND SCOPE.....	3
<b>CHAPTER 2 BACKGROUND</b> .....	<b>5</b>
2.1 RUPTURE OF INTRACRANIAL ANEURYSMS .....	5
2.1.1 <i>General information</i> .....	5
2.1.2 <i>Risk factors</i> .....	6
2.1.3 <i>Site of rupture</i> .....	7
2.1.4 <i>Size at rupture</i> .....	8
2.2 HISTOLOGY .....	10

2.3 REVIEW OF PREVIOUS RESEARCH ON INTRACRANIAL ANEURYSM RUPTURE .....	11
<b>CHAPTER 3 INTRODUCTION TO THE MODEL.....</b>	<b>14</b>
3.1 DAUGHTER ANEURYSM.....	14
3.2 LAW OF LAPLACE.....	18
3.3 AN OVERVIEW OF THE MODEL .....	20
<b>CHAPTER 4 METHODOLOGY.....</b>	<b>21</b>
4.1 ASSUMPTIONS .....	21
<i>4.1.1 Assumptions on the formation of a daughter aneurysm.....</i>	<i>21</i>
<i>4.1.2 Assumptions on the development of a daughter aneurysm .....</i>	<i>25</i>
4.2 METHOD .....	27
<b>CHAPTER 5 RESULTS.....</b>	<b>31</b>
5.1 BASIC EQUATIONS FOR DAUGHTER ANEURYSM .....	31
5.2 COMPARISON OF THE RESULTS WITH STEIGER'S COMPUTER SIMULATION.....	33
5.3 INDEX FOR ANEURYSM RUPTURE.....	35
5.4 DYNAMIC GROWTH OF DAUGHTER ANEURYSMS .....	37
5.5 TIME TO RUPTURE.....	41
<b>CHAPTER 6 DISCUSSIONS .....</b>	<b>43</b>
6.1 PATHOLOGICAL AND CLINICAL OBSERVATIONS.....	43
<i>6.1.1 Daughter aneurysm and aneurysm formation .....</i>	<i>43</i>
<i>6.1.2 Daughter aneurysm and aneurysm growth.....</i>	<i>44</i>
<i>6.1.3 Site of daughter aneurysm .....</i>	<i>45</i>
<i>6.1.4 Multiple daughter aneurysms .....</i>	<i>45</i>

6.2 DAUGHTER ANEURYSM AND ANEURYSM WALL PROPERTY.....	46
6.3 FLOW FIELD INSIDE A DAUGHTER ANEURYSM.....	47
6.4 DAUGHTER ANEURYSM: RUPTURE OR STABILIZE? .....	48
6.5 EVALUATION OF THE MODEL .....	51
6.6 LIMITATIONS/FUTURE .....	53
<b>CHAPTER 7 CONCLUSIONS AND RECOMMENDATIONS .....</b>	<b>55</b>
7.1 CONCLUSIONS .....	55
7.2 CONTRIBUTIONS.....	56
7.3 RECOMMENDATIONS .....	57
<b>REFERENCE.....</b>	<b>59</b>
<b>APPENDICES.....</b>	<b>71</b>
APPENDIX A: SOURCE CODE .....	71
<i>A.1. “draw_aneurysm.m”</i> .....	71
<i>A.2. “eta_lambda.m”</i> .....	72
<i>A.3. “two_phase_grow”</i> .....	74

## ACKNOWLEDGMENTS

First and foremost I would like to give my most sincere thanks to Dr. Hui Meng, my adviser, whose guidance and support are so critical that without them this thesis would certainly have been impossible. Her sagacity and knowledge have greatly contributed to the completion of this work. I am sure that the spiritual power I gained from her attitude and personality will benefit me enormously for the rest of my life.

My sincere thanks go to the other committee members Dr. Lee Guterman and Dr. Kenneth Hoffmann for their suggestions and objective review of my thesis.

I would particularly like to thank Dr. Ching-Shing Liu in the Mechanical Engineering Department for his patient guidance and discussions. His profound knowledge and insight have contributed greatly to this work.

I would also like to thank my fellow colleagues in the LFD and TSRC labs. Particularly, I want to mention the following names: Dr. Bernard Bendok, Dr. Ricardo Hanel, Dr. Balazs Nemes, Mr. Scott Woodward, Dr. Ye Pu, Gang Pan, Amol Mulay, Yiemeng Hoi, Zhijie Wang, Stephanie Harvey and Lujie Cao. This is a great team and I benefited enormously from it.

Last but not least, I want to thank my parents Zhenchang Feng and Jianyue Zhu for their patient understanding and love that they have generously provided me throughout my growth and education.

## NOMENCLATURE

$R$	Dome radius of parent aneurysm
$r$	Dome radius of daughter aneurysm
$a'$	Orifice radius of daughter aneurysm
$h'$	Height of daughter aneurysm
$t_d$	Wall thickness of daughter aneurysm
$t_p$	Wall thickness of parent aneurysm
$P$	Intra-aneurysmal pressure
$S_d$	Tensile stress on daughter aneurysm
$S_p$	Tensile stress on parent aneurysm
$S_0$	Wall strength of the daughter aneurysm
$\mu$	$a'/R$ , orifice index of daughter aneurysm
$\lambda$	$h'/a'$ , aspect ratio of daughter aneurysm
$\mu_0$	Initial orifice index of daughter aneurysm
$\eta$	Relative tensile stress (rupture index)
$\tau$	Non-dimensioned relative time scale
$T$	Time variable

## LIST OF FIGURES

Figure 1.1. A typical intracranial aneurysm occurring at the Circle of Willis.....	2
Figure 2.1. Aneurysm structure, morphology and histology. (From Weir B, 1985. [99])	11
Figure 3.1. Angiographs showing the presence of daughter aneurysms.....	15
Figure 3.2. A daughter aneurysm seen from CT scan.....	15
Figure 3.3. Examples of daughter aneurysms from literature. a) Two aneurysms arising at branches of a middle cerebral artery; both of them have daughter aneurysms at the fundus. (Adapted from Crawford 1959 [15].) b) Middle cerebral aneurysm which had a ruptured daughter aneurysm at the fundus. (Adapted from Crawford 1959 [15].) c) Middle cerebral artery aneurysm showing daughter aneurysms. The smaller daughter aneurysm at the fundus has ruptured. (Adapted from Crawford 1959 [15].) d) CTA study obtained in a patient with a BA tip aneurysm. (Adapted from Tateshima <i>et al</i> 2001. [90]).....	16
Figure 3.4. Illustration of the Law of Laplace in a sphere (Adapted from <a href="http://hyperphysics.phy-astr.gsu.edu/hbase/ptens.html">http://hyperphysics.phy-astr.gsu.edu/hbase/ptens.html</a> ).....	19

Figure 4.1. Force balance of the daughter aneurysm.....	23
Figure 4.2. Diagram of the model we use: a spherical aneurysm with a spherical daughter aneurysm.....	27
Figure 4.3. Illustration for the derivation of the formulas. A is the area which forms a daughter aneurysm and b is defined as a control of A, but B does not form a daughter aneurysm.....	28
Figure 4.4. Geometric relationship inside the daughter aneurysm sphere.....	30
Figure 5.1. Rupture index ( $\eta$ ) as a function of the aspect ratio ( $\lambda$ ) of the daughter aneurysm.....	32
Figure 5.2. Left: Rupture index ( $\eta$ ) as a function of the aspect ratio ( $\lambda$ ) of the daughter aneurysm at $\mu = 0.2$ . Right: Development of a daughter aneurysm: result from Steiger's computer simulation. (Adapted from Steiger 1990 [84]) .....	34
Figure 5.3. Various aneurysm geometries at rupture as predicted by the rupture index $\eta = 1$ .....	36
Figure 5.4. Orifice index vs. aspect ratio for daughter aneurysm rupture. This chart can be used to assess rupture risk of aneurysms with daughter aneurysms based on their shapes.....	37
Figure 5.5. Diagram of the development of a daughter aneurysm with $\mu = 0.2$ (rupture occurs at $\eta = 1$ ). The cartoons illustrate the shape of the aneurysm during different stages.....	40

Figure 5.6. Diagram showing the comparison of the development of aneurysms with different initial orifice indices $\mu = 0.1$ , $\mu = 0.2$ and $\mu = 0.4$ . The cartoons illustrate the shape of the aneurysms when they rupture, which occur at $\eta = 1$ .....	40
Figure 5.7. Time to rupture as a function of the orifice index of daughter aneurysm. ....	41
Figure 6.1. Schematic diagram of the intra-aneurysmal flow field with a daughter aneurysm at the dome. (Adapted from Ujiie <i>et al</i> , 1999 [96].).....	47
Figure 6.2. Various shapes of daughter aneurysms at their stable equilibrium as predicted from this model. ....	50
Figure 6.3. Different zones of daughter aneurysm as predicted by this model. ....	51

## **ABSTRACT**

Rupture of intracranial aneurysm is of primary concern to neurosurgeons. Knowledge about the rupture of intracranial aneurysms can greatly help in the decision of clinical intervention. By constructing a biomathematical model, this study proposes a rupture mechanism based on the concept of daughter aneurysm. This study discusses the formation of a daughter aneurysm, the tensile stress evolution of a daughter aneurysm and the time frame for a daughter aneurysm to rupture. Two conditions are responsible for the formation of a daughter aneurysm: local wall weakness and intra-aneurysmal pressure surge. The tensile stress on the daughter aneurysm relative to its wall strength is found to decrease first and then increase again, which suggests that daughter aneurysm may form to temporally protect itself from rupture. Based on this evolution pattern of the tensile stress on the daughter aneurysm wall, a rupture index is established within the scope of our model, which can be used to predict the rupture of an intracranial aneurysm. The time frame involved in the rupture of an intracranial aneurysm is also explored by assuming a two-phase growth pattern for the daughter aneurysm. The time to rupture is found to be closely related to the initial orifice index in our model. Although this is only a first-order model, this model helps us to understand certain phenomena of aneurysm growth and rupture. Although the final validity of this model can only be ascertained in

an *a posteriori* manner, it is believed that this model potentially can improve our understanding in the mechanism of intracranial aneurysm formation and rupture, help in evaluating the rupture potential of an intracranial aneurysm and aid in clinical decisions. Future work includes a statistical study of daughter aneurysms, use of solid modeling and analysis of the stability of the daughter aneurysm system.

# CHAPTER 1 INTRODUCTION

## 1.1 Intracranial Aneurysms

Intracranial aneurysm is a form of cerebrovascular disease characterized by the small, thin-walled ballooning, which usually occurs at the Circle of Willis (Figure 1.1). A fully developed intracranial aneurysm typically ranges in size from a few millimeters to 25 mm [33]. Current research favors a degenerative etiology of intracranial aneurysms and points to the important role that hemodynamics plays in all developmental stages of an intracranial aneurysm [81, 83]. The mechanism for the growth and rupture of an intracranial aneurysm remains elusive. Subarachnoid hemorrhage (SAH) associated with aneurysmal rupture is a potentially lethal event with a mortality rate of as high as 50% [99]. Unfortunately, most intracranial aneurysms are asymptomatic, i.e., they do not produce symptoms in patients and are discovered typically on an incidental basis or until they have already ruptured [35, 99]. The three most commonly used techniques to diagnose an intracranial aneurysm are conventional angiography, MRA, and helical (spiral) CTA. Treatment of an intracranial aneurysm includes microsurgical clipping,

embolization with Guglielmi Detachable Coils (GDC), stenting, stent-assisted coiling and liquid embolic agents.

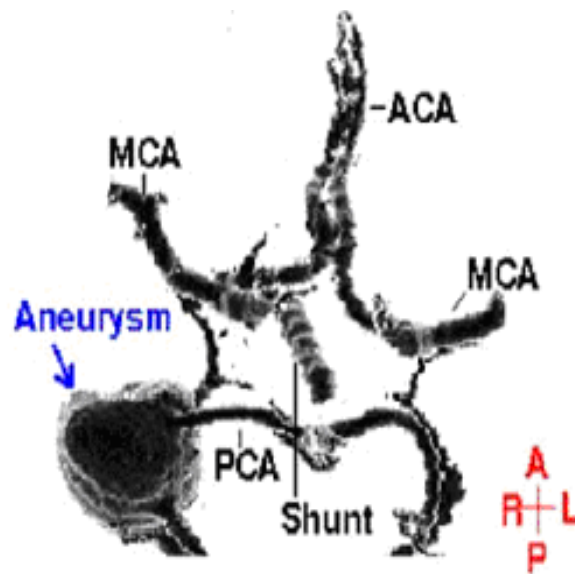


**Figure 1.1. A typical intracranial aneurysm occurring at the Circle of Willis.**

## 1.2 Mathematical Modeling

A model is a representation of a system, which can be objects, processes, or anything else we wish to describe or whose patterns of behavior we wish to analyze [24]. A mathematical model of a system is a symbolic representation involving an abstract mathematical formulation [31, 61]. Since the representation of a system contains no more information than the system it represents, a model is only as valid as the assumptions employed in its derivation.

Mathematical modeling is a powerful tool in the research of intracranial aneurysms. Previous work of mathematical modeling on aneurysm rupture is summarized in Section 2.3.

Desirable characteristics in a paper on modeling have been summarized by Yates [104] and were re-emphasized by Massoud *et al* [57]. These features include:

- 1) The model is presented with all equations demonstrated in full;
- 2) All parameters of the model are defined and their units made clear;
- 3) All equations are consistent in their dimensions and can be verified by the reader;
- 4) Data from the real system being modeled are offered to validate the model;
- 5) The domain of real time wherein the simulation is intended to be valid is given;
- 6) Any assumptions about the structure, parameter values, initial conditions, etc., are justified by carefully checked citations;
- 7) The model is clearly presented, its interesting points are highlighted, and its validation is properly documented.

### **1.3 Objectives and Scope**

The objective of this study is to provide a possible mechanism for the rupture of intracranial aneurysms. Due to the complexity and highly *in vivo* nature of the problem, mathematical modeling is employed as a primary research tool. Based on literature review and clinical evidence, this study proposes that the formation, development and rupture of a daughter aneurysm is a mechanism for the rupture of an intracranial aneurysm. Within this frame, the current study tries to address the following questions:

- (1) What are the factors involved in the formation of a daughter aneurysm?

(2) How does the wall tensile stress change with the development of a daughter aneurysm?

(3) What are the possible growth patterns for a daughter aneurysm?

(4) How to predict the rupture of an intracranial aneurysm using this model?

Finally, this study examines the assumptions of this model and discuss its validity and application in a broader pathophysiological context. Experimental evaluation of this model is not done but is discussed in the current work.

## **CHAPTER 2      BACKGROUND**

### **2.1 Rupture of Intracranial Aneurysms**

#### ***2.1.1 General information***

When an intracranial aneurysm ruptures, it bleeds into the subarachnoid space, and there is often massive hemorrhage into the brain substance and the ventricular system [83]. This event is termed as subarachnoid hemorrhage (SAH), a fatal disease which accounts for 20% of all stroke cases. The burst of an intracranial aneurysm is the primary cause to SAH. In North America, approximately 28,000 aneurysms rupture each year and roughly 50% die within the first 30 days following rupture [34, 35]. The mortality rate for aneurysm-related SAH ranges from 30% to 60%, and of those who survive, approximately 50% are left disabled [74]. The so-called “rule of five” states that if 5 patients with primary SAH from rupture of an aneurysm are left untreated, at the end a year only one will be alive and well, another will be disabled and 3 will be dead [19]. The risk of aneurysm rupture may be even larger than previously reported based on a study of Tsutsumi *et al* [94].

Despite the great morbidity and mortality rate of aneurysm rupture, there is little information available on the growth and rupture of intracranial aneurysms [83, 99]. The enlargement of an aneurysm sac appears to be highly non-uniform. Both the growth rate and the dimensions are irregular [3, 20, 21, 50, 72, 77, 87, 101]. Although it is believed that 98% of the intracranial aneurysms do not rupture [65], it is more appropriate to regard all aneurysms as being in varying stages of their development, which will in all probability lead to rupture or thrombosis [83].

### ***2.1.2 Risk factors***

Risk factors for aneurysm rupture include the following:

- 1) Cigarette smoking [45, 47, 48, 101];
- 2) Alcohol consumption [45];
- 3) Gender [4, 36, 48, 101];
- 4) Age [4, 36, 47, 102];
- 5) Symptomatic in nature [23, 101];
- 6) Hypertension [4, 15, 45, 51, 101];
- 7) Number of aneurysms [23, 101];
- 8) Aneurysm size [4, 23, 36, 45, 47, 65, 69, 101, 102, 103];
- 9) Aneurysm location [4, 36, 65, 69, 101];
- 10) Aneurysm morphology [4, 13, 27, 36, 69, 97];
- 11) History of previous SAH [23, 45, 79];
- 12) Aneurysm wall thickness [13, 27, 90];
- 13) Structural components of the aneurysm wall [27];

- 14) Flow and pressure conditions (hemodynamics) [27, 32, 77, 81];
- 15) Contact with the perianeurysmal environment [71, 77].

In order to predict the rupture potential of an intracranial aneurysm, it is also necessary to have a good understanding of the mechanism of aneurysm rupture [98]. However, the mechanism of aneurysm growth and rupture is still obscure. Among the four stages of an aneurysm “life cycle” (genesis, development, thrombosis and rupture), rupture is the least understood one. Compared with the large body of literature on unruptured aneurysms, there is little documentation on the mechanism of aneurysm rupture. A summary of previous research on aneurysm rupture is presented in this thesis. (See Section 2.3)

### ***2.1.3 Site of rupture***

Hademenos *et al* reported that posterior circulation aneurysms have a higher risk of rupture [36]. Weir *et al* found that 40.3% of the ruptured aneurysms were on the anterior cerebral artery (ACA) or anterior communicating artery (AComA). Aneurysms in the basilar artery (BA) bifurcation also had a greater tendency than those in the middle cerebral artery (MCA) to rupture [102]. In the famous “International Study of Unruptured Intracranial Aneurysms” (ISUIA) [45], two groups were gathered retrospectively. In the group of patients with no history of SAH, only 10% were AComA and 23% were MCA lesions. In the other group with previous SAH, only 8% were AComA and 38% were MCA aneurysms. This suggests that the site of aneurysm rupture may be related with the anatomy of the Circle of Willis and the different local hemodynamic parameters.

Within an aneurysmal sac, rupture occurs almost invariably at the fundus where the flux of blood entering the sac impinges on the wall [84]. Crompton studied 289 cases and found that 84% ruptured through the apex, 14% ruptured through the body and only 2% ruptured through the neck [16]. Unfortunately he did not give the information about the specific type of the ruptured aneurysms. In a pathological study performed by Crawford, he localized the rupture site to the fundus or apex in 64% of the cases, 10% to the middle third of the sac and only 2% to the neck or proximal third of the sac (the location of the other 24% was undetermined) [15]. The high frequency of rupture at the fundus supports the use of surgical clipping as a common treatment for intracranial aneurysms. One interesting phenomenon is that, contrary to the common impression that the dome is the thinnest part of an aneurysm sac, it was found that the neck was thinner than the dome [90]. This suggests that the rarity of rupture at the neck must be explained on the basis of hemodynamic factors [77].

#### ***2.1.4 Size at rupture***

In general, it may be said that the larger the aneurysm, the greater is the tendency to rupture. The mean size of all ruptured aneurysms was significantly larger than the mean size of all unruptured aneurysms [102]. Most cerebral aneurysms are between 5 and 10 mm in diameter when they rupture. Unruptured aneurysms are generally less than 6 mm in external diameter, and in practice the risk of hemorrhage seems to be greater with increasing size of the aneurysm [16, 83, 90].

The critical size for intracranial aneurysms has long been an issue of controversy. Whether intracranial aneurysms reach a certain size before they rupture is still not

established yet [85]. The conclusion varies from author to author. Some authors reported that unruptured intracranial aneurysms smaller than 1 cm have a very low probability of rupture [45, 103]. Some believe that the majority of aneurysms rupture at an average diameter of less than 1 cm [16, 28, 49]. McCormick studied the sizes of 140 aneurysms and concluded that an aneurysm less than 5 to 6 mm is unlikely to rupture [56]. But Kassell studied 1092 patients and found that over 10% were less than 5 mm in diameter [49]. Crompton also found that the majority of the ruptured aneurysms were about 5 mm. The critical size is between 2 and 5 mm [16]. It was also reported that tiny aneurysms of less than 3 mm can rupture and cause the so-called “benign SAH” [85, 90, 105].

The inconsistency of these data may result from the following facts. 1) It is inappropriate to compare the size of an aneurysm that has already been ruptured with that of an unruptured one. There has been evidence that many aneurysms decrease in size after rupture [20]. 2) It is possible that there are overwhelmingly more small aneurysms than large aneurysms. As a result, a small portion of ruptured small aneurysms may represent a big portion of the total ruptured aneurysms. 3) Since all aneurysms are at continuous development, it is possible that the investigation of aneurysm size is influenced by the time of measurements, especially considering that aneurysm growth is very unpredictable [3, 20, 21, 50, 72, 77, 87, 101].

The controversy regarding the critical size of aneurysm rupture suggests that size alone is not an adequate factor to predict aneurysm rupture.

## 2.2 Histology

Since intracranial aneurysms differ anatomically from normal vasculature, it is useful to review the histology of normal arteries and intracranial aneurysms. Normal arteries are consisted of three distinct layers: tunica intima, tunica media and tunica adventitia [77]. Compared with their extracranial counterparts, intracranial arteries are characterized by an attenuated tunica media and adventitia, and no external elastic lamina (EEL). Intracranial aneurysm wall has a very thin tunica media or none, and the internal elastic lamina (IEL) is either absent or severely fragmented [1, 72]. Thus, it is generally composed of only intima and adventitia [74]. (See Fig. 2.1) Collagenous connective tissue is the dominant component of an intracranial aneurysm wall [40]; components such as elastin and smooth muscle are present in negligible amount in an intracranial aneurysm wall [73] and therefore do not make a significant contribution to its wall mechanics. Thus, it can be concluded that the mechanical properties of an aneurysm are mainly related to the fiber strength and orientation of collagen [55]. Loss of elastin can also explain why intracranial aneurysms are considerably less distensible than normal cerebral arteries [76].

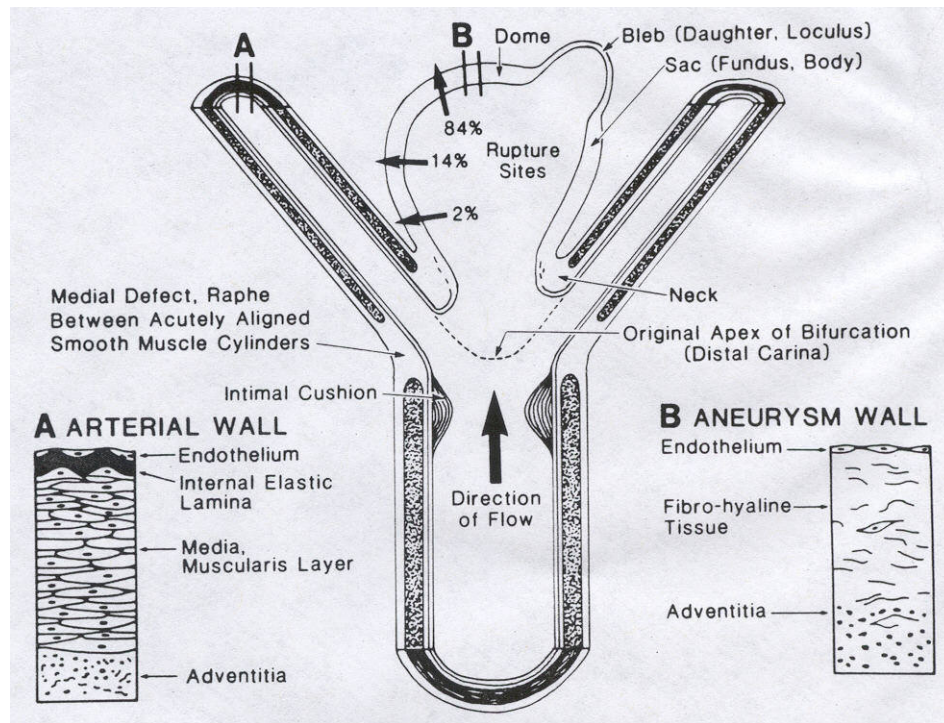


**Figure 2.1. Aneurysm structure, morphology and histology. (From Weir B, 1985. [100])**

### **2.3 Review of Previous Research on Intracranial Aneurysm Rupture**

Despite of its importance, there has been only limited research on the rupture of intracranial aneurysms. While it is known that hemodynamics plays an important role in the rupture of intracranial aneurysms, aneurysm rupture cannot be explained by hemodynamic factors alone. One must consider both aneurysm hemodynamics and the wall properties. It is often suggested that aneurysms rupture when the local wall tensile stress exceeds its wall strength [77], but how the local wall tensile stress gets to exceed the wall strength and what steps are included in this process are still unknown. In history, several mechanisms have been postulated to explain the rupture mechanism of intracranial aneurysms, but none of them is satisfactory.

One theory of rupture states that with the onset of wall failure, the wall yields and further enhances the tension according to the Law of Laplace (See Section 3.2), thus instigating a vicious cycle – the greater the wall tension, the more the wall expands; and the more the wall expands, the greater is the wall tension [27]. There are some drawbacks of this theory. 1) It assumes that expansion of the aneurysm will cause thinning of the aneurysm wall. This is not true. On the contrary, aneurysm wall thickness increases with the increase of aneurysm radius [58, 83, 85] as a result of wall remodeling [12]; 2) It cannot explain why most intracranial aneurysms do not rupture.

Jain postulated a rupture mechanism based on his experimental model of a latex aneurysm sac attached to a lateral tube in a closed circuit with pulsatile flow. He concluded that resonance phenomenon could occur in aneurysms and cause aneurysm rupture [46]. However, Steiger reviewed the significance of periodic flow and concluded that aneurysmal vibrations induced by periodic flow appeared to be small and they only represented an epiphenomenon with limited importance for aneurysm growth and rupture [85].

Austin and colleague suggested that an increase in pulse pressure or pulse rate can result in increased turbulence, which is a destructive factor on the aneurysm wall leading to sudden enlargement and potential rupture [6, 7, 8]. But whether the flow inside an intracranial aneurysm is turbulent or laminar is still not established. In fact, many results showed that the flow inside an aneurysm is rather predictable instead of being turbulent [17, 88]. Steiger, after careful review, suggested that the flow field inside intracranial aneurysms depends on several factors including the shape and size of an aneurysm, aneurysm wall elasticity and Reynolds number [85].

Because of the highly complex *in vivo* nature involved in the process of aneurysm rupture, mathematical modeling remains a most commonly used tool. The purposes of using mathematical models to simulate intracranial aneurysms were described in the work of Hademenos *et al* [37, 38]. One of the most well-known models is established by Canham and Ferguson, where they estimated the critical size at rupture by adopting the Law of Laplace [13]. Hung and Botwin applied the thin-shell theory to a spherical model and found that the natural frequencies of some aneurysms fall within the range of bruit frequencies that commonly accompany aneurysms [44]. Nieto and Torres constructed a nonlinear mathematical model that simulated the blood flow inside an aneurysm [63]. Austin used an electric circuit model and found that an increase in pulse pressure or pulse rate can result in increased turbulence, which is a destructive factor on the aneurysm wall leading to sudden enlargement and potential rupture [7]. Hademenos and colleagues modified the Law of Laplace and established nonlinear mathematical models for both saccular [37] and fusiform intracranial aneurysms [38]. Chitanvis *et al* developed a nonlinear constitutive quasi-static model and studied the dynamic behavior of saccular aneurysms in response to pulsatile blood flow [14]. More recently, Dickey and Kailasnath hypothesized that rupture risk varies as the third power of aneurysm diameter based on their assumption that the likelihood of an aneurysm rupture is proportional to the number of weak spots in an aneurysm wall [18]. These mathematical models, while not perfect, provide us with qualitative and/or quantitative information and valuable insight into the rupture of intracranial aneurysms.

## **CHAPTER 3      INTRODUCTION TO THE MODEL**

### **3.1 Daughter Aneurysm**

The sudden enlargement or surface bubbles on an intracranial aneurysm wall are commonly termed as “daughter aneurysms” [16, 70]. Daughter aneurysms are often observed clinically, and many researchers have reported them using the term “daughter aneurysm” [16, 69, 70, 75, 97], “surface bubble” [16], “loculation” [7, 22, 42, 50], “lobulation” [1, 2, 5, 72, 89], “secondary loculus” [20, 26], “bleb” [15, 30, 41, 59, 62, 85, 91, 92, 95, 98], “daughter sac” [23, 75], “outpouching” [64], “multilobed” [4, 36], or “multichamber” [42]. Figure 3.1 – 3.3 are examples of clinically observed daughter aneurysms.



**Figure 3.1. Angiographs showing the presence of daughter aneurysms.**

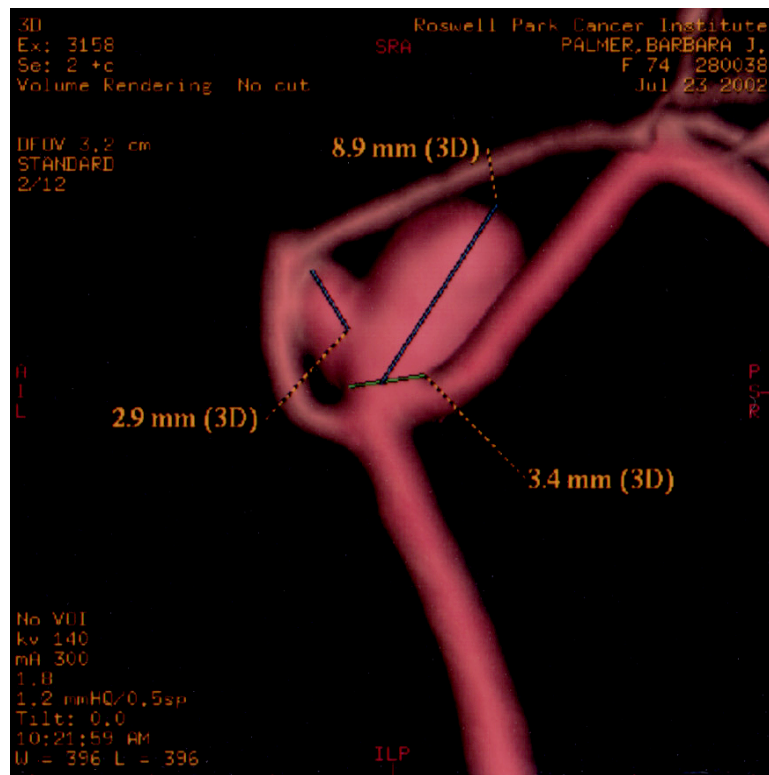


**Figure 3.2. A daughter aneurysm seen from CT scan.**

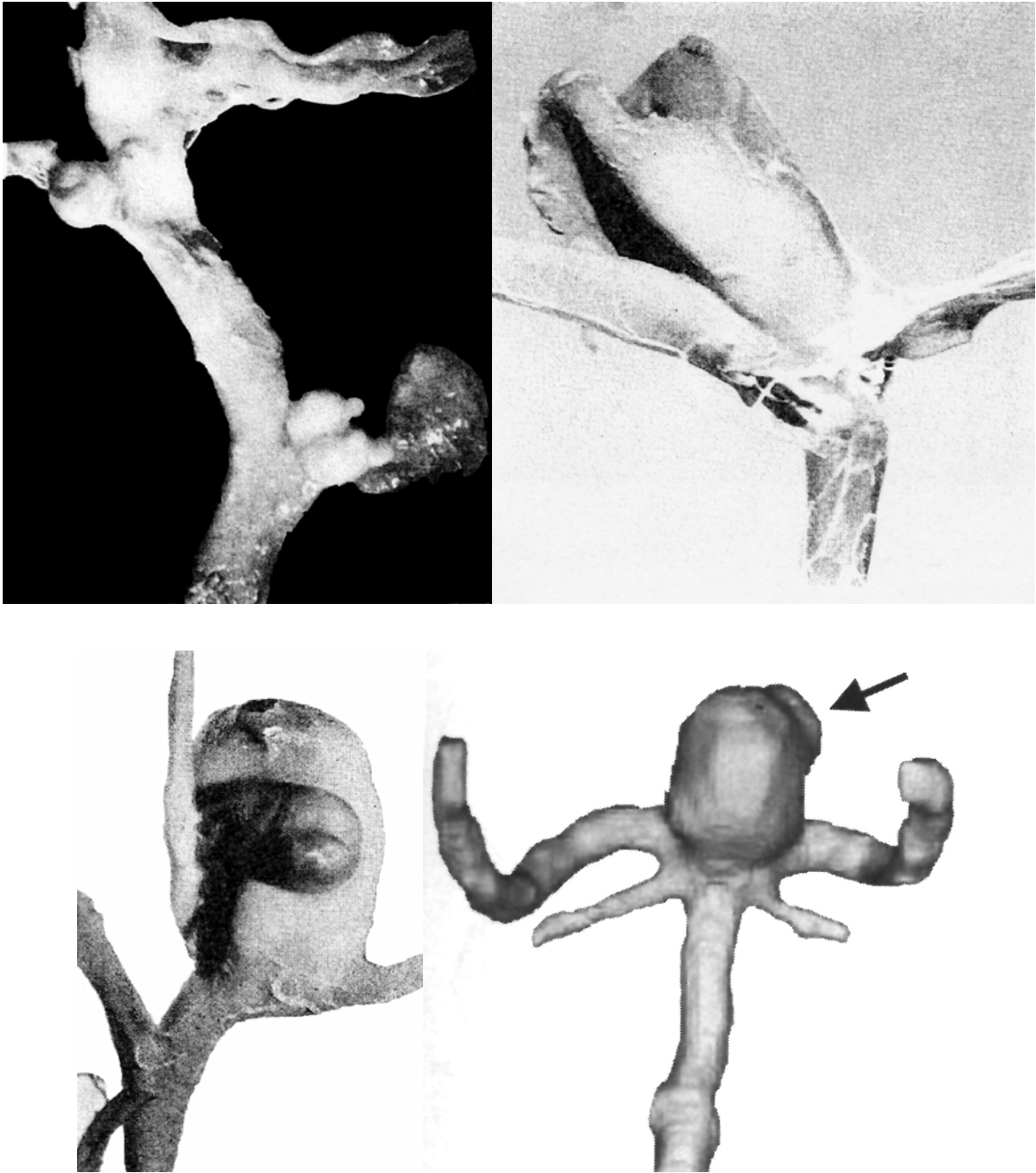


**Figure 3.3. Examples of daughter aneurysms from literature. a) Two aneurysms arising at branches of a middle cerebral artery; both of them have daughter aneurysms at the fundus. (Adapted from Crawford 1959 [15].) b) Middle cerebral aneurysm which had a ruptured daughter aneurysm at the fundus. (Adapted from Crawford 1959 [15].) c) Middle cerebral artery aneurysm showing daughter aneurysms. The smaller daughter aneurysm at the fundus**

**has ruptured. (Adapted from Crawford 1959 [15].) d) CTA study obtained in a patient with a BA tip aneurysm. (Adapted from Tateshima *et al* 2001. [91])**

Back in 1966, Crompton performed a pathological study of 275 ruptured intracranial aneurysms and found that 57% of the aneurysms had daughter aneurysm “bubbles”. In contrast, only 16% of 112 unruptured aneurysms had a bubble on the surface [16]. In a study by Sampei *et al*, three of four unruptured aneurysms with a daughter aneurysm later ruptured between 1 month and 10 years of follow-up review, whereas only 2 of 10 unruptured aneurysms without a daughter aneurysm later ruptured [70]. Austin also reported the formation of one or more loculations, which he interpreted as abrupt enlargement due to a focal weakening in the wall [7]. In a cerebral angiographic study by Hinshaw and colleagues, one third of the aneurysms were found to be loculated and 65% of these patients had SAH [42]. Du Boulay studied the natural history of intracranial aneurysms and found that over one third of the recent bled aneurysms had one or more loculus, whereas aneurysms not responsible for recent bleedings had virtually no loculus [20]. Although Chitanvis *et al* [14] did not include daughter aneurysm in their modeling, they particularly pointed out that “...undulations in the aneurysm wall could play an important role in the path to rupture”. These reports strongly suggest that daughter aneurysms are associated with aneurysm rupture. Clinically, surgeons tend to treat an intracranial aneurysm more urgently if a daughter aneurysm is observed [23]. It has been suggested that aneurysms harboring daughter aneurysms should be treated or at least be followed up with MRI [67]. Therefore, it is important that we consider the daughter aneurysm phenomenon when modeling aneurysm rupture.

Besides angiographic and autopsy studies discussed above, it was shown in Steiger's computer simulation of the development of cerebral aneurysms that an aneurysm could gain new stability by forming a bleb or daughter aneurysm at the weaker part of the wall [85]. This is in agreement with Austin's arguments, which he asserted that the "loculations" represent a second stable equilibrium after the initial enlargement [7].

Despite the fact that daughter aneurysms are commonly known to neurosurgeons, there has been little research done to explain quantitatively the existence of daughter aneurysms. To the best of our knowledge, Steiger is the only one who explained the daughter aneurysm phenomenon by using the Law of Laplace in his computer simulation of aneurysm development [85]. It is believed in this study that the daughter aneurysm phenomenon is so important to aneurysm rupture that a systematic investigation is needed.

### **3.2 Law of Laplace**

The Law of Laplace describes the relationship between the circumferential stress and the radius for any curved elastic surface. According to the Law of Laplace, the tension in the wall of a hollow sphere is computed as:

$$T = PR/2 \quad [\text{Eq. 3.1}]$$

where T is the tangential tension on the wall, P is the intramural pressure, and R is the radius of curvature. For a cylinder, the formula is:

$$T = PR \quad [\text{Eq. 3.2}]$$

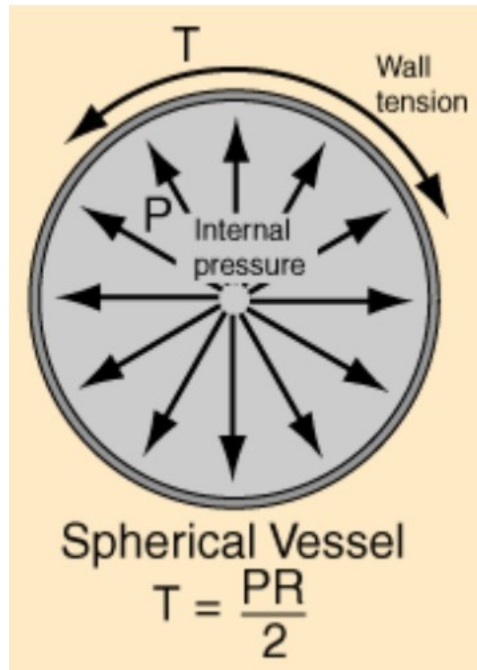


**Figure 3.4. Illustration of the Law of Laplace in a sphere (Adapted from <http://hyperphysics.phy-astr.gsu.edu/hbase/ptens.html>)**

The derivation of this law can be found in many books and papers [13, 25, 34]. It should be noted that the above expression for the Law of Laplace is valid only for thin-walled elastic structures, i.e.,  $t \ll R$ , where  $t$  is the thickness of the vessel wall.

The tensile stress ( $S$ ) of an arterial wall is defined as the tension per unit cross-section of the vessel wall. It is dependent on the wall tension and wall thickness:

$$S = PR/t \quad [\text{Eq. 3.3}]$$

The Law of Laplace, despite its simplicity, is a powerful tool in modeling many biological and pathophysiological phenomena [25].

### 3.3 An overview of the Model

This study has developed a mathematical model on the rupture of intracranial aneurysms, where we propose that the formation, development and rupture of daughter aneurysm is a mechanism for the rupture of an intracranial aneurysm. The formation of a daughter aneurysm is a combined result of intra-aneurysmal pressure surge and local wall weakness, and it is related to the distribution of the properties of the aneurysm wall. The relative tensile stress  $\eta$  of the daughter aneurysm wall depends on two parameters: its orifice index  $\mu$  and its aspect ratio  $\lambda$ . In our model, as a daughter aneurysm develops,  $\eta$  first decreases to its minimal value (at  $\lambda = 0.577$ ) and then increases again until it reaches the value of 1. According to our model, since the daughter aneurysm grew out of the weakest part of the wall and it was about to rupture before it forms, it will rupture before or at  $\eta = 1$ . Thus  $\eta$  can be served as a rupture index in this model. The growth mode cannot be derived from this model itself, but it is hypothesized that the growth mode of a daughter aneurysm involves two phases: a fast phase followed by a slow phase. The end of the fast phase is likely to be a stable equilibrium for the daughter aneurysm. Further studies may involve a statistical study of daughter aneurysms in terms of their morphology, histology and mechanical properties; stability analysis of the daughter aneurysm system to study the condition why some daughter aneurysms are in stable equilibrium while others rupture; and solid modeling of the daughter aneurysm model using more realistic geometries.

## CHAPTER 4 METHODOLOGY

### 4.1 Assumptions

The model is based on the following assumptions.

#### *4.1.1 Assumptions on the formation of a daughter aneurysm*

This study proposes that the formation of a daughter aneurysm is the result of pressure surge inside the aneurysmal sac and the existence of a “weak” area in the aneurysm wall. Before the pressure surge, this “weak” area has deteriorated to such a degree that it can hardly withstand the tensile stress and is just about to rupture. Then it responds passively to the intra-aneurysmal pressure surge and develops a daughter aneurysm out of this “weak” area. Here the “weak” part of the aneurysm wall is characterized by its low Young’s Modulus, which is defined as

$$Y = \frac{F}{A \cdot \Delta L / L_0}$$

where  $F$  is force,  $A$  is the cross-sectional area of the aneurysm strip,  $L_0$  is the initial length and  $\Delta L$  is the change in length.

- **Driving force**

The driving force for the formation and development of a daughter aneurysm is the intra-aneurysmal pressure. The local wall weakness responds to the pressure surge by forming a daughter aneurysm. Factors that can cause the intra-aneurysmal pressure changes include systemic blood pressure, intracranial pressure, size and shape of the aneurysm, diameter and length of the parent artery, intra-aneurysmal flow field, aneurysm wall properties and vasospasm [79]. Intra-aneurysmal pressure surge is possible under certain pathophysiological circumstances. Austin postulated that “jump phenomenon” can occur in intra-aneurysmal pulse pressures with small increases in systemic pulse pressure or pulse rate [7]. Foutrakis *et al* suggested that impingement of the flow can greatly increase the pressure gradient at the aneurysm apex [29]. Higher intra-aneurysmal pressure may also be induced by downstream stenosis. In an experiment by Sekhar and colleagues, intra-aneurysmal pulse pressure exhibited a cubic relationship with mean arterial pressures (MAPs) after a 50% stenosis [78]. Injection of contrast medium during angiography can also elevate intra-aneurysmal pressure. It was reported that intra-aneurysmal systolic pressure can increase by 5-23 mmHg immediately after injection of contrast medium [79]. An electric shock may also cause a sudden rise in blood pressure and induce intracranial aneurysm rupture [80].

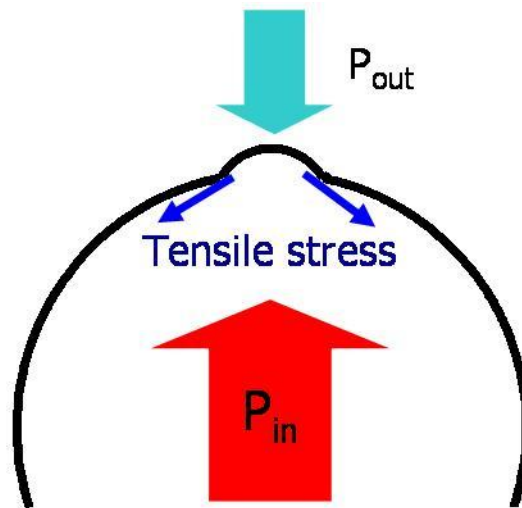


**Figure 4.1. Force balance of the daughter aneurysm.**

- **Local wall weakness**

Steric inhomogeneities in the viscoelastic properties of human intracranial aneurysms have been observed and may play an important role in their development and rupture [93, 94]. One of the factors that will affect the Young's Modulus is the thickness of the aneurysm wall; namely the thinner the wall, the smaller the Young's Modulus. It has been reported that the thickness of an aneurysm wall varies within the aneurysmal sac, especially for large aneurysms [87]. Some parts of the wall consist of only a thin layer of fibrous tissue and endothelium, while some other parts consist of fibromuscular tissue [83]. Mizoi and colleagues reviewed 78 cerebral aneurysms and found that 50% of them had partially thin-walled sac at the dome [58]. It was reported that persistent thin-walled areas of aneurysms lacking the normal structural elements accounts for SAH that occurs in up to 36% of patients with giant aneurysms [87].

Weakening of an aneurysmal wall may be caused by a number of pathophysiological and/or hemodynamic factors. Histologically, loss of smooth muscle cells (SMC) and derangement of connective tissue elements will lead to deterioration of the aneurysm wall strength [93]. It has been reported that fatty plaques and/or calcifications can weaken the aneurysm wall and lead to local outpouchings which are prone to rupture [64]. The stagnant intra-aneurysmal flow field may cause inadequate nutrition for collagen synthesis and maturation, weakening of the elastic membrane and collagen, which result in weakening of the aneurysm wall [42, 72]. Intra-aneurysmal turbulence was observed by several authors and was believed to be able to cause the degeneration of elastica [26, 27, 39]. Jet impinging on the dome of an aneurysm may also cause the fatigue of the local aneurysm wall [83, 84]. High pressure also appears to break the single elastin layer of cerebral arteries [84] and cause infiltration of atheromatous plaques [64].

The weaker part of the parent aneurysm can also be the result of a previous hemorrhage. Saccular aneurysm-like bled formation after aneurysm rupture has been reported by Hayashi *et al* [41]. It is known that there is a substantial difference between previously ruptured and unruptured aneurysms [70, 103]. Suzuki and Ohara observed that intracranial aneurysms can stop bleeding soon after aneurysm rupture and form a new protective fibrin layer, which is relatively weaker than the original aneurysmal wall [90]. Fibrin deposition leading to local wall weakness is also discussed by Steinburg and Chung [87]. Formation of a daughter aneurysm bleb after a previous rupture has been documented by Hayashi *et al* [41]. It is likely that the aneurysm wall forms another protective layer after the daughter aneurysm ruptured, which would represent a repeated

rupture at this site, but since the daughter aneurysm wall is already very weak, the new protective layer cannot survive long.

#### ***4.1.2 Assumptions on the development of a daughter aneurysm***

The following assumptions made are made on the development of a daughter aneurysm:

- 1) *Both the parent aneurysm and daughter aneurysm are spherical.* A spherical shell is believed to be a reasonable approximation to an intracranial aneurysm [14, 66, 99, 100]. There is little documentation on the geometry of daughter aneurysms. From our observation of a few angiographs, a daughter aneurysm usually appears as spherical or elliptical.
- 2) *The aneurysm wall is thin as compared with the radius, such that the Law of Laplace can be applied.* Intracranial aneurysm wall is known to be very thin [50, 77, 85, 90]. In one report, the average intracranial aneurysm wall thickness is 51  $\mu\text{m}$  [1]. And it appeared from measurements that the thickness of the aneurysm walls amounted to about 2.4% of the radius of the aneurysms [85]. This is good enough for the application of the Law of Laplace. But it was also reported that the thickness of the aneurysm wall could be as large as the thickness of normal cerebral artery, which is around 1 mm [83]. In these rare cases, application of the Law of Laplace will introduce significant errors.
- 3) *The pressure on the daughter aneurysm wall and the pressure on other parts of the aneurysm wall are identical.* Computer Fluid Dynamics (CFD) simulation by Mulay *et al* show that the pressure distribution inside an aneurysmal sac is rather

homogeneous except for the distal neck region where a higher pressure is observed [59].

- 4) *New tissue is added to the parent aneurysm and to the daughter aneurysm at the same rate.* The fourth assumption is important in that it allows the thickness of the aneurysm wall to increase during the development of the daughter aneurysm. Although some authors have assumed a constant aneurysm wall volume in their modeling processes [13, 27, 85], it is believed in this study that tissue remodeling is important during the development of an intracranial aneurysm. It has been found that aneurysm wall thickness increases with the enlargement of the aneurysm radius [58, 83, 85]. This is a reflection of the fact that aneurysms wall is capable of responding to its environment and is capable of repairing itself [10, 12, 101], as Crompton has pointed out that "... the wall of an aneurysm is a living and metabolizing structure, able to add to and reinforce itself. Enlargement does not necessarily imply thinning." [16] Remodeling of the aneurysmal wall structure was also emphasized by Ujiie *et al* and was believed to be involved in the mechanism of aneurysm rupture [98]. Studies have shown that tissue remodeling of intracranial aneurysms is closely related with the remodeling process of extracellular matrix (ECM), which is a dynamic network of proteins and proteoglycans [51]. Collagen is the predominant element in the ECM of an intracranial aneurysm wall. During remodeling of ECM, new collagen is proliferated and differentiated, and the cross-linkage of collagen is also altered, which can change the tensile strength of an aneurysm wall [51].

- 5) *The growth of daughter aneurysm in the width direction is negligible compared with the height direction.* This assumption is rather conceptual and it is based on our assumption that daughter aneurysm forms at the weak part of an aneurysm wall. It is assumed that this weak part does not increase during the development of daughter aneurysm. To the best of our knowledge, there has been no documentation on the dynamic growth of a daughter aneurysm.

## 4.2 Method

According to the assumptions, a graphic model is presented in Figure 4.2. In this figure,  $R$  and  $r$  is the radius of the parent aneurysm and the daughter aneurysm, respectively;  $a'$  is half of the length of the daughter aneurysm orifice which is also referred as “orifice radius” in following sections;  $h'$  is the height of the daughter aneurysm measured from the base.

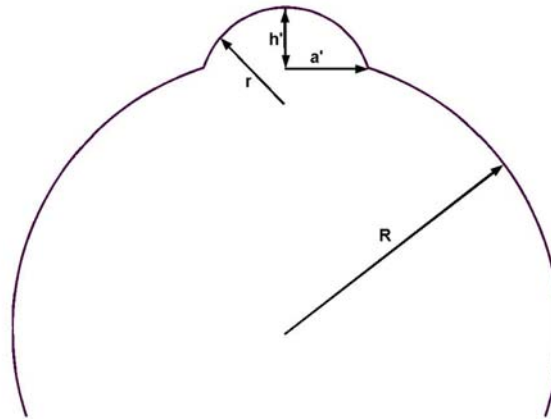


**Figure 4.2. Diagram of the model we use: a spherical aneurysm with a spherical daughter aneurysm.**

Here this study looks at the change of the wall tensile stress (S) during the development of a daughter aneurysm, because the tensile stress in an aneurysm wall is known to be the predominant force responsible for aneurysm growth and rupture [1, 9, 12, 26, 27, 81].

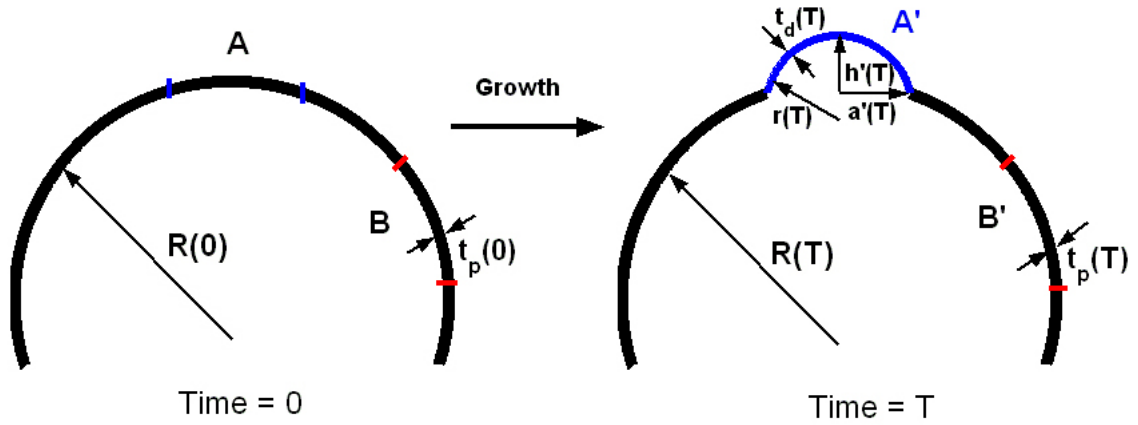


**Figure 4.3. Illustration for the derivation of the formulas. A is the area which forms a daughter aneurysm and b is defined as a control of A, but B does not form a daughter aneurysm.**

Figure 4.3 illustrates the dynamic process of daughter aneurysm development. It is assumed that initially (at time 0), the area which is going to develop a daughter aneurysm is of thickness  $t_p(0)$ . And this study conceptually defines a control area B which is identical to area A at time 0, but it does not develop a daughter aneurysm. This study does this simply for the purpose of illustration.

Applying assumption (4), the volume of B' and A' should be the same:

$$2\pi R(T) \cdot \{R(T) - \sqrt{[R(T)]^2 - [a'(T)]^2}\} \cdot t_p(T) = 2\pi r(T) \cdot h'(T) \cdot t_d(T) \quad [\text{Eq. 4.1}]$$

where  $R(T)$  is the radius of the parent aneurysm at time  $T$ ,  $a'(T)$  is the base radius of the daughter aneurysm at time  $T$ ,  $h'(T)$  is the height of the daughter aneurysm at time  $T$ ,  $t_p(T)$  is the thickness of area B', and  $t_d(T)$  is the thickness of area A'. The left hand side of the equation is the volume of area B', and the right hand side is volume of area A'.

Equation 4.1 can be rearranged as below:

$$\frac{t_d(T)}{t_p(T)} = \frac{R(T)}{r(T)} \cdot \frac{R(T) - \sqrt{[R(T)]^2 - [a'(T)]^2}}{h'(T)} \quad [\text{Eq. 4.2}]$$

According to assumption (1) and (2), the Law of Laplace (See Section 3.2) can be applied to both the parent aneurysm and the daughter aneurysm, which yields:

$$S_d(T) = \frac{P(T) \cdot r(T)}{2 \cdot t_d(T)} \quad [\text{Eq. 4.3}]$$

and

$$S_p(T) = \frac{P(T) \cdot R(T)}{2 \cdot t_p(T)} \quad [\text{Eq. 4.4}]$$

We then define the relative tensile stress  $\eta(T) = \frac{S_d(T)}{S_p(T)}$ , with  $S_d(T)$  and  $S_p(T)$  being

the tensile stress on the daughter aneurysm and on the parent aneurysm at time  $T$ , respectively. It will be shown later in this model that  $\eta$  can serve as a rupture index of the aneurysm.

Dividing Eq. 4.3 by Eq. 4.4 yields

$$\frac{t_d(T)}{t_p(T)} = \frac{r(T)}{R(T)} \cdot \frac{S_p(T)}{S_d(T)} = \frac{r(T)}{R(T)} \cdot \frac{1}{\eta(T)} \quad [\text{Eq. 4.5}]$$

Combining Eq. 4.5 and Eq. 4.2 yields:

$$\eta(T) = \left[ \frac{r(T)}{R(T)} \right]^2 \cdot \frac{h'(T)}{R(T) - \sqrt{R^2 - a'^2}} \quad [\text{Eq. 4.6}]$$

Notice that in the daughter aneurysm sphere, the following geometrical relationship exists as is shown in Eq. 4.7. (Figure 4.4):

$$[r(T) - h'(T)]^2 + [a'(T)]^2 = [r(T)]^2 \quad [\text{Eq. 4.7}]$$

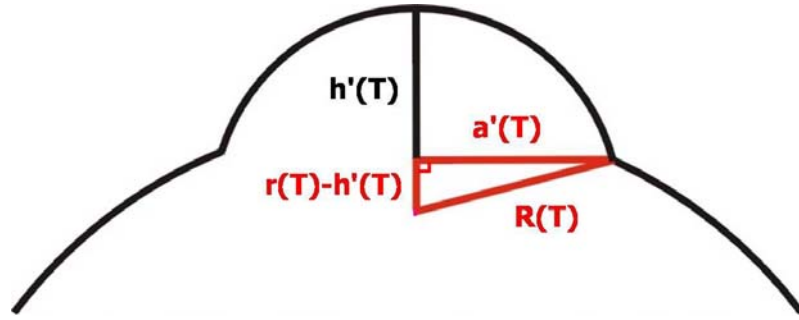


**Figure 4.4. Geometric relationship inside the daughter aneurysm sphere.**

Equation 4.7 is equivalent to:

$$[a'(T)]^2 + [h'(T)]^2 = 2r(T) \cdot h'(T) \quad [\text{Eq. 4.8}]$$

From Eq. 4.6 and Eq. 4.8, it is obtained that

$$\eta(T) = \eta[\mu(T), \lambda(T)] = \frac{\mu(T) \cdot [1 + \sqrt{1 - \mu(T)^2}]}{4} \cdot \frac{\{1 + [\lambda(T)]^2\}^2}{\lambda(T)} \quad [\text{Eq. 4.9}]$$

where  $\mu(T) = \frac{a'(T)}{R(T)}$  is the orifice index, indicating the relative size of the daughter

aneurysm orifice (neck) as compared to the size of the parent aneurysm, and  $\lambda(T) = \frac{h'(T)}{a'(T)}$

is the aspect ratio of the daughter aneurysm, indicating the basic shape of the daughter aneurysm.

## CHAPTER 5 RESULTS

### 5.1 Basic Equations for Daughter Aneurysm

As introduced before, wall tensile stress is the predominant force responsible for aneurysm rupture [1, 9, 12, 26, 27, 81], hence this study focuses on the change of the tensile stress of the daughter aneurysm,  $\eta$  is expressed as a function of  $\mu$  and  $\lambda$ :

$$\eta(\lambda, \mu) = \frac{\mu(1 + \sqrt{1 - \mu^2})}{4} \cdot \frac{(1 + \lambda^2)^2}{\lambda} \quad [\text{Eq. 5.1}]$$

In Eq. 5.1, the relative tensile stress on the daughter aneurysm is expressed as a function of two dimensionless shape parameters:  $\mu$  is the orifice of the daughter aneurysm nondimensioned by the radius of the parent aneurysm; and  $\lambda$  is the aspect ratio of the daughter aneurysm defined as height normalized by the orifice radius.

Equation 5.1 illustrates the dependence of the tensile stress of daughter aneurysm on two shape parameters; thereby it serves as a basis for rupture risk assessment. It also provides a scheme to characterize a daughter aneurysm by the measurable non-dimensioned shape parameters, therefore enable us to study the daughter aneurysm model in a systematic approach.

The dependence of the relative tensile stress  $\eta$  on aspect ratio  $\lambda$  at various orifice index  $\mu$  levels is plotted in Figure 5.1. For a fixed  $\mu$ , the relative tensile stress  $\eta$  reaches its minimum at  $\partial\eta/\partial\lambda = 0$ , which gives an aspect ratio of  $\lambda = \sqrt{3}/3 \approx 0.577$ . Note that before the daughter aneurysm initiates, it is part of the parent aneurysm wall, having the same tensile stress as the parent aneurysm ( $\eta = 1$ ). Hence all the curves start from  $\eta = 1$ .

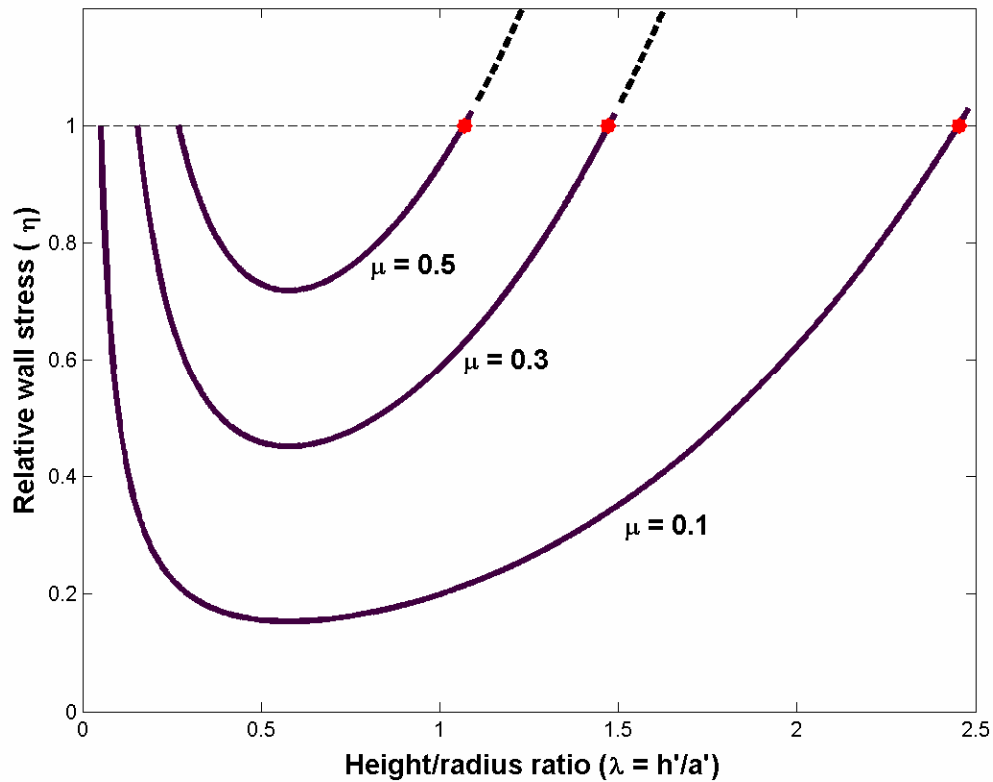


**Figure 5.1. Rupture index ( $\eta$ ) as a function of the aspect ratio ( $\lambda$ ) of the daughter aneurysm.**

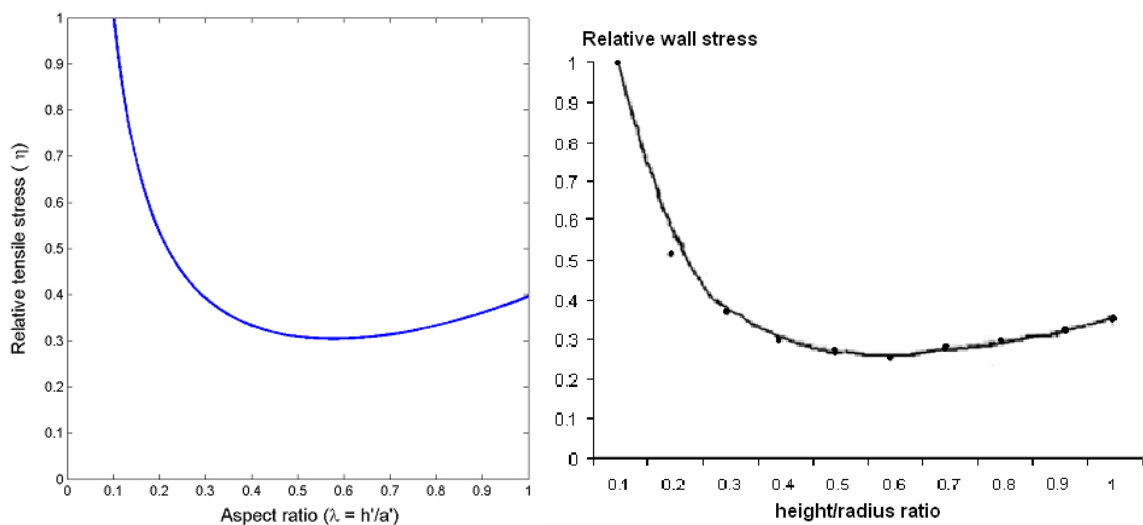
It helps us understand the physics behind these curves in Figure 5.1 by analyzing the process during the development of a daughter aneurysm. The growth process of a daughter aneurysm is characterized by two simultaneous processes: 1) Change of the spherical radius  $r$ . As a daughter aneurysm develops, its spherical radius first decreases

until the bulge reaches a semi-spherical shape ( $\lambda = 1$ ) and then increases. 2) Thinning of the daughter aneurysm wall due to the volume restriction of the wall material. As a result of these two processes, the relative tensile stress on the daughter aneurysm first decreases and then increases again.

Figure 5.1 suggests that the formation of a daughter aneurysm works to protect the weak part of the aneurysm wall from rupture by temporarily reducing its tensile stress.

## 5.2 Comparison of the Results with Steiger’s Computer Simulation

For comparison, Figure 5.1 is re-drawn using  $\mu = 0.2$  and  $\lambda$  from 0 to 1. The results from Steiger [85] is shown in Figure 5.2 right, where the “relative wall stress” first decreases and then increases with the height/radius ratio in a very similar manner as curves in Figure 5.1 computed from Eq. 5.2. Although in Steiger’s paper the “relative wall stress” was not explicitly defined, its name suggests that this quantity is similar to the relative tensile stress  $\eta = S_d/S_p$  defined in our work.



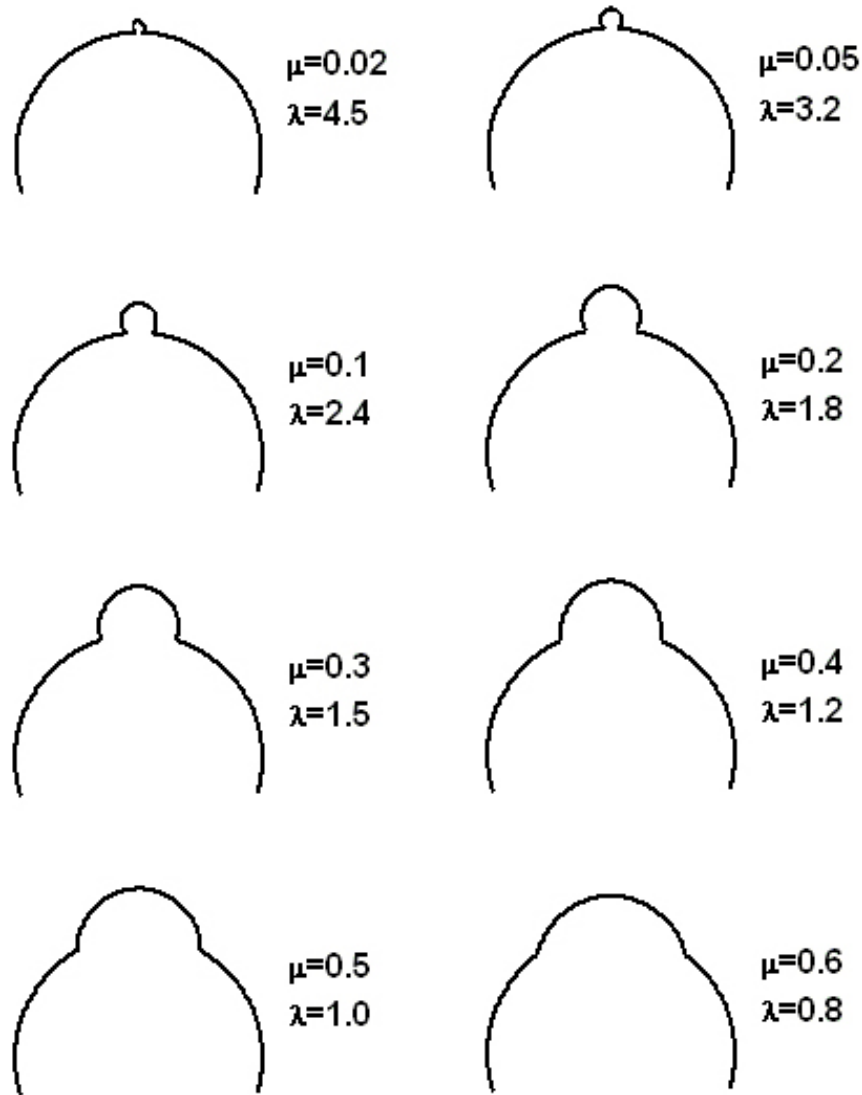
**Figure 5.2. Left: Rupture index ( $\eta$ ) as a function of the aspect ratio ( $\lambda$ ) of the daughter aneurysm at  $\mu = 0.2$ . Right: Development of a daughter aneurysm: result from Steiger's computer simulation. (Adapted from Steiger 1990 [85])**

Figure 5.2 indicates that the results of this study agree well with Steiger's computer simulation. Both show the transitional height/orifice-radius value to be 60%, but this study does not agree with his statement that daughter aneurysms tear if they grow higher than that point. In fact, daughter aneurysms with aspect ratios of greater than one are commonly observed clinically, especially for those with small orifice indices (Figure 3.3 a). Although the relative tensile stress begins to increase beyond that point, we can see from Figure 5.1 that  $\eta$  is still smaller than 1 for most curves (for example, the curve  $\mu = 0.5$ ), which means that the stress on the daughter aneurysm is still smaller than that on the parent aneurysm. (Remember that  $\eta$  is the ratio between the tensile stress on the daughter aneurysm and that on the main aneurysm). Rupture will occur, however, when the wall of the daughter aneurysm cannot endure the tensile stress on it. As part of the assumption for the formation of a daughter aneurysm, the wall of a daughter aneurysm is weaker than other parts of the aneurysm wall, so when the tensile stress on the daughter aneurysm becomes the same as other parts of the wall ( $\eta = 1$ ), the probability for the rupture of the daughter aneurysm increases and the whole aneurysm may rupture. The use of relative tensile stress as a rupture index in our model is further discussed in the next section.

### 5.3 Index for Aneurysm Rupture

$\eta = 1$  is chosen to be a criterion for aneurysm rupture because daughter aneurysm was formed when that part of the wall could not endure the high local tensile stress. As shown in Figure 5.1, the development of daughter aneurysm temporarily reduces the tensile stress ( $\eta < 1$ ), but as the relative tensile stress increases and it reaches 1 again, the weaker part of the wall is again subject to the same tensile stress as before the daughter aneurysm was formed. Theoretically it is possible to grow a “grand daughter aneurysm”, but clinically there has been no report on this phenomenon. Since the daughter aneurysm wall is already weaker than other parts, its strength cannot be more than the original strength  $S_0$ , hence it is expected that the daughter aneurysm to rupture when  $S_d = S_0$ . Thus,  $\eta = 1$  serves as an indication for rupture, and this is a rather conservative estimation. A more accurate rupture index can be adopted based on the wall strength of a specific daughter aneurysm. For example, for a daughter aneurysm whose wall strength is half of that of the parent aneurysm wall, it is more reasonable to use  $\eta = 0.5$  as its rupture index.

Using  $\eta = 1$  as a rupture index, this study can obtain different shapes of daughter aneurysms when they are expected to rupture. Figure 5.3 shows several examples of them. The clinical significance of these aneurysms shapes is obvious: aneurysms of such shapes are likely to rupture at any time.



**Figure 5.3. Various aneurysm geometries at rupture as predicted by the rupture index  $\eta = 1$ .**

Since in this model the geometry of daughter aneurysm is characterized by its orifice index  $\mu$  and aspect ratio  $\lambda$ , this study further explores the relationship with respect to these two shape factors at rupture. In Figure 5.4, the “rupture line” represents all the daughter aneurysms when they are expected to rupture as predicted by this model. Below

the rupture line is the “unruptured zone”, in which the daughter aneurysms are still unruptured; and on top of the line is the “ruptured zone”, in which daughter aneurysms should have already ruptured as predicted by this model. This plot provides us with a means to assess the rupture risk of an aneurysm by measuring the orifice index and aspect ratio of its daughter aneurysm.

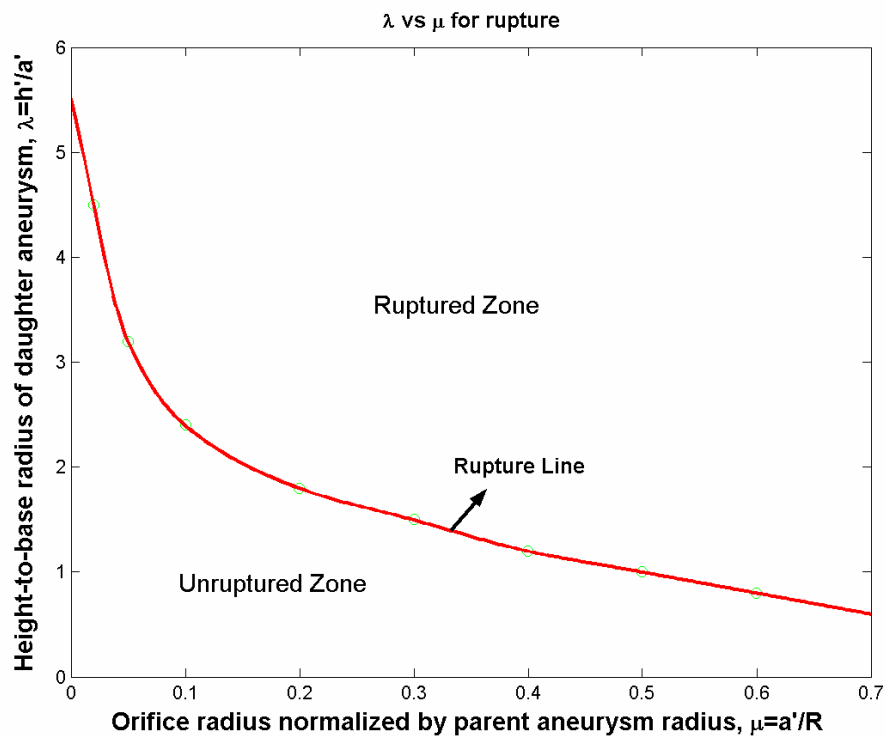


**Figure 5.4. Orifice index vs. aspect ratio for daughter aneurysm rupture. This chart can be used to assess rupture risk of aneurysms with daughter aneurysms based on their shapes.**

## 5.4 Dynamic Growth of Daughter Aneurysms

For an aneurysm in the “unruptured zone” with a certain risk of rupture, it is of great interest to further predict how much time is left before it ruptures, or whether it will

reach that point at all. This requires a model that describes the dynamic growth of daughter aneurysm as a function of time. The modeling of the actual change of  $\lambda$  and  $\mu$  with time requires detailed simulations of the aneurysms wall dynamics and active tissue remodeling. This study assumes a simple growth mode, in which assumes  $\mu$  remains constant and  $\lambda$  increases linearly with time during the daughter aneurysm growth. The growth in height (or  $\lambda$ ) has two phases. The first phase is identified as “fast phase”, during which period the daughter aneurysm expands rapidly until  $\eta$  reaches its minimal point (Figure 5.1). The second phase is called “slow phase”. During this phase, the daughter aneurysm grows linearly in height until it ruptures. This growth mode is qualitatively consistent with our common observation of the outburst of a bulge on a balloon or rubber tire. However, it is purely conceptual and experimental proof is needed.

From Figure 5.1, the tensile stress on the daughter aneurysm decreases during the first phase. This means there is less and less resistance to the growth of the daughter aneurysm as the daughter aneurysm enlarges. This positive-feedback process accounts for the rapid growth during the first phase. During the second phase, the tensile stress on the daughter aneurysm increases, providing a negative feedback to its further growth, meaning that growth becomes more and more “difficult”. This may account for the slow growth rate of the second phase.

The total time for a daughter aneurysm to rupture is the summation of the time involved in the first phase and the duration of the second phase, i.e.,  $\tau_r = \tau_1 + \tau_2$ , where  $\tau_r$  is the time to rupture,  $\tau_1$  is the time involved in the first phase and  $\tau_2$  is the time involved in the second phase. Since the growth in the fast phase is rapid, a further assumption is

made that the duration of the first phase is negligible as compared with that of the second phase, i.e.,  $\tau_1 \ll \tau_2$ . Therefore,  $\tau_r \approx \tau_2$ .

The growth of daughter aneurysm during the second phase is mathematically described as follows:

$$\begin{cases} \mu(\tau) = \mu_0 = \text{Constant} \\ \lambda(\tau) = \sqrt{3}/3 + (1-\sqrt{3}/3)\tau \end{cases} \quad [\text{Eq. 5.2}]$$

$$\eta(\tau) = \frac{\mu(1+\sqrt{1-\mu^2})}{4} \cdot \frac{[1+\lambda(\tau)^2]^2}{\lambda(\tau)} \quad [\text{Eq. 5.3}]$$

where  $\tau$  is time scaled by the time it takes for the daughter aneurysm to develop into a hemisphere. The slope  $(1-\sqrt{3}/3)$  and  $\tau$  are chosen in such a way that if the daughter aneurysm grows continuously with this rate, it will take  $\tau = 1$  to develop into a hemisphere.

A plot of this growth mode (for  $\mu = 0.2$ ) is shown in Figure 5.5.

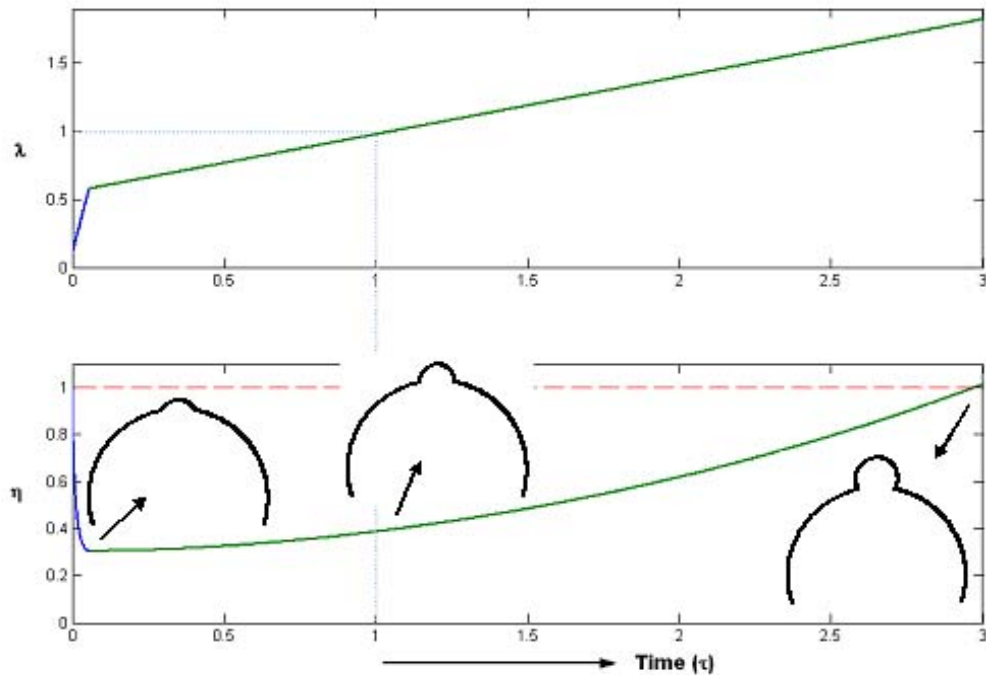


**Figure 5.5. Diagram of the development of a daughter aneurysm with  $\mu = 0.2$  (rupture occurs at  $\eta = 1$ ). The cartoons illustrate the shape of the aneurysm during different stages.**

Using the same methodology, this study can also plot the growth of daughter aneurysms with different initial orifice indices  $\mu$ 's. (Figure 5.6)

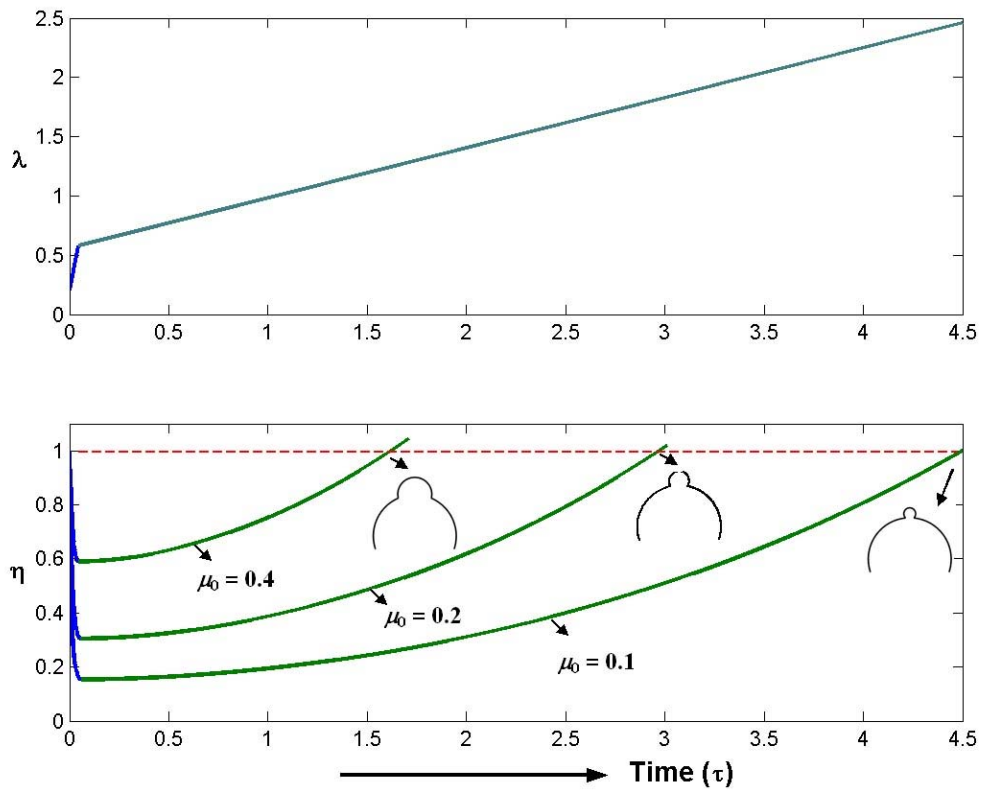


**Figure 5.6. Diagram showing the comparison of the development of aneurysms with different initial orifice indices  $\mu = 0.1$ ,  $\mu = 0.2$  and  $\mu = 0.4$ . The cartoons illustrate the shape of the aneurysms when they rupture, which occur at  $\eta = 1$ .**

## 5.5 Time to Rupture

Given the model on the dynamic growth of daughter aneurysm, this study further explores the relationship between the time to rupture and the orifice index  $\mu$ . From Figure 5.6, it can be inferred that for a given growth mode, the time for an aneurysm to rupture is a function of the orifice index  $\mu$  only (since a unique growth mode is assumed). Following the same growth mode as described in Section 5.4, the relationship between the time to rupture and the orifice index  $\mu$  of the daughter aneurysm can be plotted.

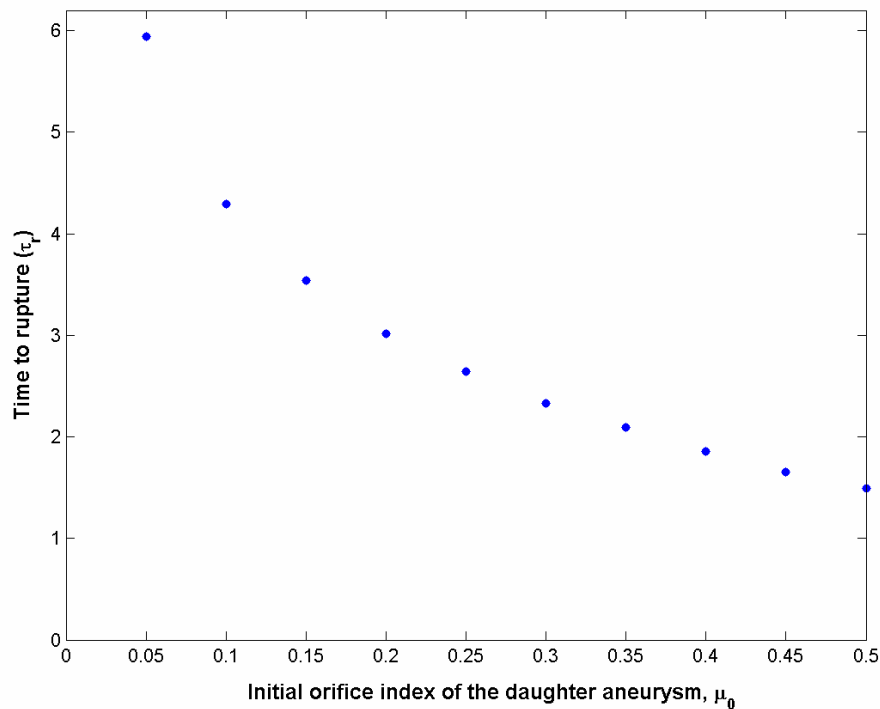


**Figure 5.7. Time to rupture as a function of the orifice index of daughter aneurysm.**

Figure 5.7 shows clearly that the time to rupture decreases as the initial orifice index increases. While the actual growth mode and the point of rupture may differ from the assumed, the general trend shown by this curve should remain the same. This has

been tested by assuming several different growth modes for daughter aneurysms. For example, in one growth mode it is assumed that the daughter aneurysm first grows in height with its base kept constant until it is about to rupture, and then the base expands with the height fixed until it is about to rupture, and this process goes on. Since the initial orifice index is an indication of the percentage of the “critical weaker areas” of the aneurysm wall in which daughter aneurysm may form, it follows that the larger the weaker area, the sooner an aneurysm will rupture. This conclusion, consistent with some experimental studies [1, 77, 90], may provide insight into the rupture of intracranial aneurysms.

## **CHAPTER 6      DISCUSSIONS**

### **6.1 Pathological and Clinical Observations**

This section discusses the existence of daughter aneurysms in more details and explores it the context of aneurysmal pathophysiology, biology and hemodynamics.

#### ***6.1.1 Daughter aneurysm and aneurysm formation***

Taking the concept of daughter aneurysm to the extremity, we might view the cerebral artery as the parent aneurysm in our model, and then the development of a daughter aneurysm would be analogous to the genesis of an intracranial aneurysm. Stehbens has identified three early changes related to the development of saccular aneurysms: funnel-shaped dilatations, areas of thinning and microscopic evaginations [82]. This supports that daughter aneurysms will develop out of the weaker part of the wall, which is characterized by gross thinning of the wall, gross deficiency of the elastica and media. But the structure of an aneurysm wall is different from that of the normal cerebral arterial wall. The aneurysmal sac itself usually is composed only of intima and

adventitia, while the media is absent [74]. In early aneurysm formation, the bulging is from the luminal surface into the wall of media; in daughter aneurysm formation, the bulging is mainly from the intima directly into the adventitia.

### ***6.1.2 Daughter aneurysm and aneurysm growth***

Daughter aneurysms have also been found more frequently on larger aneurysms [7], hence associating themselves with aneurysm growth. According to Stebhens, aneurysm features which may predict impending rupture are thin areas in the wall, sac-like pouches extending outward, patchy fibrin infiltration, layers of thrombus on the inner aspect of the sac, inflammatory cells in the sac wall, and blood pigment containing macrophages and erythrocytes within the wall [82]. In an immunohistochemical comparison of ruptured and unruptured aneurysms, the walls of ruptured aneurysms exhibited more significant endothelial damage, inflammatory cell invasion, and structural changes in the vessel wall. There was also a loss of smooth muscle cells and degradation in matrix proteins. Elastase and collagenase activity was higher in the walls of ruptured aneurysms [11]. It is conceivable that these enzymes participate in the erosion and thinning of the aneurysm wall hence predisposing the wall to daughter aneurysm formation. In a pathological examination of 45 aneurysms, lesions smaller than 3 mm were composed of mostly endothelial cells and fibrous tissue. Ones larger than 4 mm contained collagen in their walls and had developed thin areas in their domes [25]. These pathological and clinical observations put together suggest that daughter aneurysms are at the very least associated with aneurysm growth and rupture.

### **6.1.3 Site of daughter aneurysm**

Because daughter aneurysm is closely associated with rupture, it seems logical to reason that most daughter aneurysms grow from the dome region of the parent aneurysms, since it is found clinically that most intracranial aneurysms rupture at the fundus [77, 97]. Because the aneurysm develops out of a diseased portion of the vessel wall, its wall property is generally weaker than the normal vessel wall. There must be a continuous deterioration of the vessel wall from the parent artery to the aneurysmal wall. This deterioration is a reflection of the histology of the aneurysm wall: the media is absent. The dome region is farther off the normal artery than other parts of the aneurysm wall, thus it represents the weakest part of the aneurysm wall. Unlike the neck region, the dome does not have tissue support from the parent vessel. Weakness in the aneurysm dome may also be resulted from jet impingement, since most intracranial aneurysms are formed at vessel bifurcations. As clinical evidence, Murata *et al* reviewed operative findings of 36 patients treated with neck clipping and found that 80 % of aneurysms had thin wall domes with or without daughter aneurysms [59].

### **6.1.4 Multiple daughter aneurysms**

It is possible that another *de novo* daughter aneurysm form at a different site of the parent aneurysm wall, with the same mechanism as the formation of the first daughter aneurysm. Clinically, multiloculation has been observed by several authors [16, 42, 72]. But in this case, the process is much more complicated since the development and rupture of both daughter aneurysms have to be considered. Multiple daughter aneurysms are not as common as single daughter aneurysms and they are not studied in this work.

## **6.2 Daughter Aneurysm and Aneurysm Wall Property**

The formation of a daughter aneurysm may also be related with the aneurysm wall property itself. In 1971, Austin investigated the stress-strain and pressure-volume relationships in experimental model latex rubber aneurysms and suggested that either a high pulse rate or increased pressure may lead to a critical jump phenomenon and increased turbulence of flow within the aneurysm. In 1989, he and his colleagues used a model that mimics the elastance of fresh aneurysm walls and performed another experiment to study the contribution of pressure and volume in the enlargement of intracranial aneurysms. They found that a pressure threshold exists during the enlargement of an aneurysm. Before the threshold, there is linear enlargement in volume with increased pressure, while after the threshold, there is an abrupt jump in volume (mean increase =  $70 \pm 14$  %) to a new stable equilibrium volume. Austin also found in his electric circuit model that an increase in pulse pressure or pulse rate can result in increased turbulence, which is a destructive factor on the aneurysm wall leading to sudden enlargement and potential rupture [6]. It may be viewed from this study that the abrupt increase in volume is a sign of forming and growing daughter aneurysms. It is also concluded in the paper that a further increase in pressure could eventually result in aneurysm rupture, indicating that daughter aneurysm may be a precursor of rupture [8].

### 6.3 Flow Field Inside a Daughter Aneurysm

In this study, the impact of the flow inside an aneurysmal sac is ignored since it is known that the velocity inside an aneurysmal sac is much smaller than that of the parent vessels [54, 85, 86]. The pressure field inside an aneurysmal sac found to be nearly constant [59].

The flow field inside a daughter aneurysm was investigated by Ujiie *et al* [97] and is shown in Figure 6.1. It can be seen that the flow activity inside a daughter aneurysm is extremely sluggish. The orifice of the daughter aneurysm functioned as a second neck but of remarkably narrow size, thus severely reducing the flow. According to Bernoulli's law, the pressure inside the daughter aneurysm should be greater than that inside the parent aneurysm. It is likely this elevated pressure will contribute to the development of a daughter aneurysm.

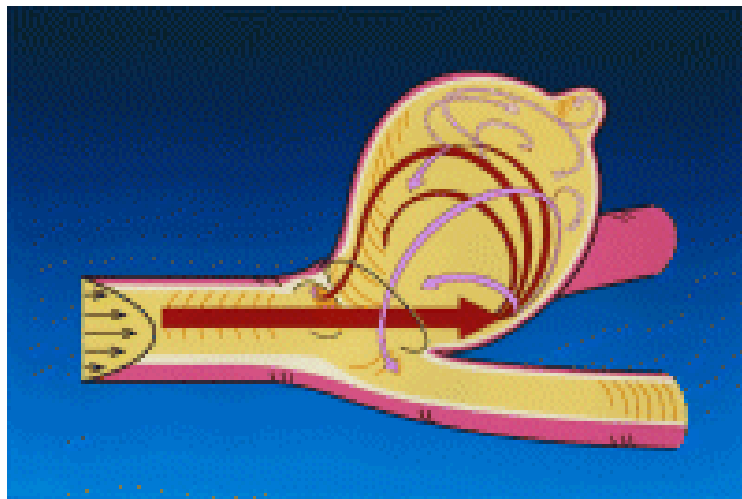


**Figure 6.1. Schematic diagram of the intra-aneurysmal flow field with a daughter aneurysm at the dome. (Adapted from Ujiie *et al*, 1999 [97].)**

In the studies of Tateshima *et al* [91, 92], wall shear stress (WSS) was calculated from the velocity gradient using laser Doppler Velocimetry (LDV) from an acrylic aneurysm model constructed from 3D CT angiography. It was found that WSS was the highest at the bleb of an aneurysm. This indicates that the increased WSS might have been involved in the development of a daughter aneurysm. This high WSS at the daughter aneurysm may destroy the endothelial cells and result in the local weakening of the aneurysm wall. Since high WSS is regarded as a major factor in the formation and development of intracranial aneurysms [52], it is likely that this elevated WSS inside a daughter aneurysm contributes to the development of the daughter aneurysm.

However, the results from Ujiie *et al* and Tateshima *et al* seem contradictory. How can the flow field inside a daughter aneurysm be extremely sluggish while having the highest WSS? This discrepancy suggests that further *in vitro* experiments are needed to study the flow field inside a daughter aneurysm. More importantly, the relationship between the intra-aneurysmal hemodynamics and the daughter aneurysm growth is to be established.

#### **6.4 Daughter Aneurysm: Rupture or Stabilize?**

While daughter aneurysms are often precursors of rupture, it should be noted that not all daughter aneurysms result in rupture. In fact, some authors reported that a daughter aneurysm represents a stable equilibrium at the weak part of an aneurysm wall [7, 8, 85]. This seemingly controversial role of daughter aneurysms can be resolved using the results and hypotheses of this model.

In section 5.4, this study made a hypothesis that the development of a daughter aneurysm involves two phases: a fast phase and a slow phase. And the change of the driving force for the daughter aneurysm as it grows was discussed during these two phases. It is possible that in some cases, the driving force at the end of the first phase may become zero. Then as the daughter aneurysm grows further, the net force on the daughter aneurysm is opposing its growth. This may be the mechanism for the daughter aneurysm to be at equilibrium or stabilize at the end the first phase. In order for the daughter aneurysm at this equilibrium to develop further, a greater pressure surge is required to overcome the increasing tensile stress. However, the mechanism for this condition remains to be elucidated, which may become possible by performing a stability analysis on the stressed daughter aneurysm model. The various geometries of the daughter aneurysms at their stable equilibrium are illustrated in Figure 6.2. This is based on the geometries of daughter aneurysms at the end of their first phase growth.

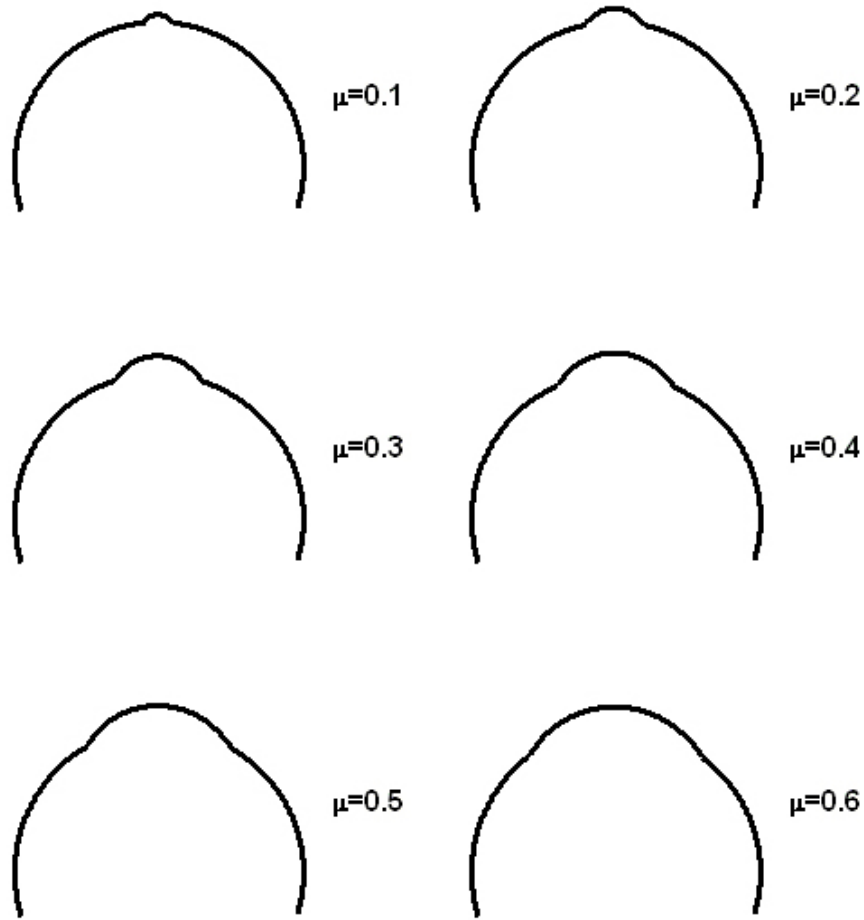


**Figure 6.2. Various shapes of daughter aneurysms at their stable equilibrium as predicted from this model.**

Our prediction is that daughter aneurysms grow beyond the shapes in Figure 6.2 is at a higher risk of rupture than those below the shapes in Figure 6.2. Clinical evidence is needed for evaluation of this hypothesis.

All the aspect ratios in Figure 6.2 are 0.577. In Figure 6.3, it is combined with the plot in Figure 5.4. Now there are three distinct zones: safety zone, transitional zone and ruptured zone. The safety zone is the region before a daughter aneurysm develops into stabilization. In this region, the daughter aneurysm is relatively “safe”. The transitional zone is the region between stabilization and rupture. Daughter aneurysms in this zone

should be followed by angiography. The rupture zone is the region above the rupture line, and daughter aneurysms in this zone should have already ruptured as predicted by this model. Like Figure 5.4, Figure 6.3 provides us with a tangible means to evaluate our model.

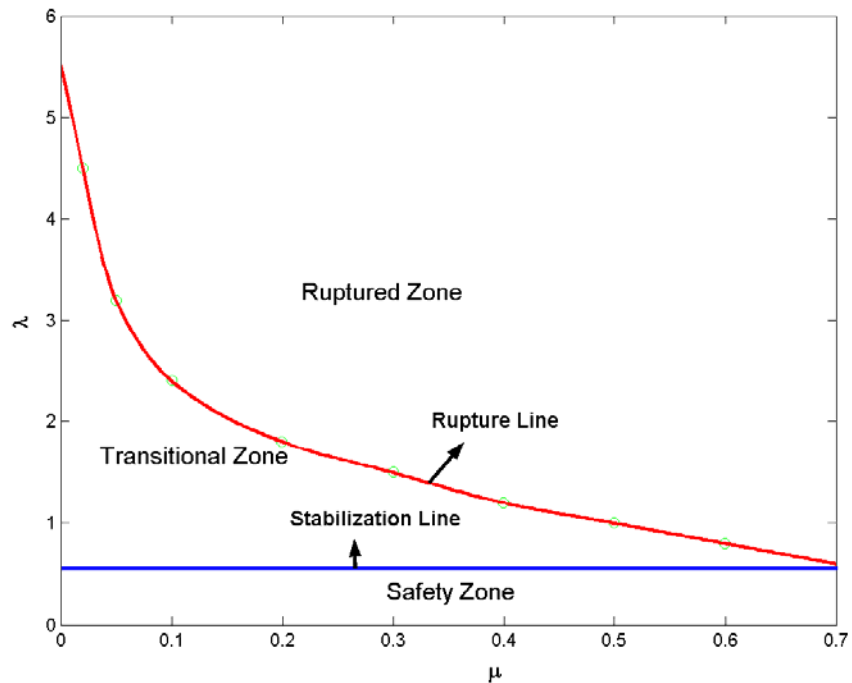


**Figure 6.3. Different zones of daughter aneurysm as predicted by this model.**

## 6.5 Evaluation of the Model

In contrast to an actual model whose performance can be evaluated by experimental examinations, a conceptual model has to rely on logic for its justification and is considered satisfactory if the mathematical formulation of its performance is identical with that of the original system [57].

Our model is consistent with some well-known phenomena in aneurysm development and rupture.

- 1) It is known that the development of intracranial aneurysms is unpredictable [3, 21, 77]. One of the reasons could be that the process of aneurysm growth can be complicated by formation and development of daughter aneurysms. Du Boulay believed that loculus of the parent aneurysm could be the reason of delayed hemorrhage [20].
- 2) Hypertension is known to be a risk factor of aneurysm rupture [4, 15, 45, 51, 101]. In our model, an increase of the pressure inside the aneurysmal sac is one of the requirements for the formation of a daughter aneurysm. The increased intra-aneurysmal pressure may be the primary driving force for the formation and development of daughter aneurysms. (Section 4.1)
- 3) It has been a confusing phenomenon that in many cases small aneurysms rupture while large aneurysms stay unruptured [75, 106]. It is conceivable that small aneurysms, irrespective of their small sizes, may have uneven wall strength distributions and grow daughter aneurysms which may lead them to rupture.
- 4) Our model is also consistent with the observation that some aneurysms with remarkably thin walls do not rupture [84]. It is likely that the thin-walled part is on a daughter aneurysm sac and is in stable equilibrium. However, in order to have a thorough understanding of the last two

phenomena, the mechanism of how daughter aneurysms stabilize has to be elucidated. (Section 6.4)

The validity of this model can in fact only be ascertained in an *a posteriori* manner, owing to the highly *in vivo* nature of the subject. A statistical study is necessary in order to compare the results of this model to the actual clinical data.

## **6.6 Limitations/Future**

There are several limitations of this model. First of all, some assumptions may not represent the actual case and will affect the modeling results. For example, it is assumed that a daughter aneurysm maintains a spherical shape during its development. In fact, elliptic daughter aneurysms are commonly observed. Second, the model does not predict the exact time frame over which rupture will occur. The model also neglects biological processes such as enzymatic erosion of the wall, and it assumes steady-state, i.e., neglecting the pulsatile nature of the hemodynamic forces. Furthermore, it does not establish the mechanism why some daughter aneurysms lead to rupture while some remain in stable equilibrium.

Despite these limitations, it is believed that this model may provide a new framework for understanding aneurysm rupture. Given the complexity and multifactorial nature of aneurysm growth and rupture, it is unlikely that one mathematical model will characterize the behavior of all intracranial aneurysms. This model, rather, may help understand one of several ways an aneurysm can rupture. The usefulness of this model

will ultimately depend on evaluations by *in vitro* and *in vivo* experiments, which aim to understand aneurysm rupture.

Future work will include solid modeling of the daughter aneurysm model. This would allow us to use more realistic daughter aneurysm geometries and incorporate aneurysm wall properties. Stability analysis of the daughter aneurysm model is needed in order to find out the mechanism for the stability of daughter aneurysms. A statistical study of daughter aneurysms is also important in order to obtain the geometry distribution of daughter aneurysm, wall properties of a daughter aneurysm and the time frame for a daughter aneurysm to develop and rupture.

# CHAPTER 7      CONCLUSIONS AND RECOMMENDATIONS

## 7.1 Conclusions

This study proposes that the formation, development and rupture of a daughter aneurysm is involved in the mechanism of intracranial aneurysm rupture. The formation of a daughter aneurysm is a combined result of intra-aneurysmal pressure surge and weakened aneurysm wall, and it is related to the distribution of the properties of the aneurysm wall. The relative tensile stress  $\eta$  of the daughter aneurysm wall depends on two parameters: its orifice index  $\mu$  and its aspect ratio  $\lambda$ . As the daughter aneurysm develops,  $\eta$  first decreases to its minimal value (at  $\lambda = 0.577$ ) and then increases again until it reaches the value of 1. Since a daughter aneurysm was formed when that part of the wall has deteriorated to such a degree that it was about to rupture, and the wall of a daughter aneurysm is originally weaker than other parts of the parent aneurysm, it is expected that it will rupture before or at  $\eta = 1$ , when the tensile stresses on the daughter aneurysm becomes the same as before the daughter aneurysm is formed. Thus  $\eta$  is used

as an index for rupture in this model. In order to study the dynamic growth of a daughter aneurysm, it is further hypothesized that the development of a daughter aneurysm involves two phases: a fast phase and a slow phase. Based on this hypothesis and the rupture index  $\eta$ , this study establishes the time frame for a daughter aneurysm to rupture. The time for an aneurysm to rupture is found to be highly dependent on the initial orifice index. This model is consistent with some observations in the growth and rupture of intracranial aneurysms. However, more experimental and clinical data are needed in order to evaluate this model.

## **7.2 Contributions**

While the validation of this model can only be ascertained in an *a posteriori* manner, this study improves our understanding in the mechanism of aneurysm rupture, which is still obscure to us. Our study emphasizes the predictive value of a daughter aneurysm in the rupture of an intracranial aneurysm. Instead of focusing on size alone of an intracranial aneurysm to evaluate its rupture risk, it is suggested by this model to look at factors that are involved in the formation and development of daughter aneurysms. The conclusions of our study produce understanding and insights to the rupture of an intracranial aneurysm, such as the importance of the “initial orifice index” in determining the time to rupture. These conclusions, if carefully evaluated, can help in the screening and decision of treatment for intracranial aneurysms. The current study also shows the necessity to build a database of intracranial aneurysms with manifestation of daughter aneurysms. Such a database can be used to determine which type of intracranial aneurysms is more likely to grow daughter aneurysms, the actual geometry of daughter

aneurysms, the hemodynamic parameters involved in daughter aneurysm development, and the time frame for a daughter aneurysm to develop and rupture...

### **7.3 Recommendations**

The current study emphasizes the importance of the properties of an aneurysm wall in predicting its rupture risk. Instead of only looking at the size of an aneurysm, it is suggested that it is more important to focus on factors that are involved in the formation and development of a daughter aneurysm. Size is one of the factors that will influence the growth of a daughter aneurysm, namely the larger the radius, the more likely a daughter aneurysm will grow. Other factors include area of local wall weakness, intra-aneurysmal pressure change etc.

This study shows a necessity to build a database of intracranial aneurysms with manifestation of daughter aneurysms. While it is still difficult to directly analyze the focal fragility of the aneurysmal wall, an estimation based on its shape is possible [98]. Such a database could be used to determine which specific type of parent aneurysms is more likely to grow daughter aneurysms, the actual geometry of daughter aneurysms, the hemodynamic parameters involved in daughter aneurysm development, and the time period for a daughter aneurysm to grow and rupture.

One of the challenges in establishing a daughter aneurysm database is the inadequate ability of imaging devices to detect the presence and shape of aneurysm lobulation, which can be as small as 1 mm. Even the enhanced MRA is not adequate for detection of lobulation of an intracranial aneurysm [5]. Recent progress in digital subtraction angiography (DSA) shows that it is significantly superior to detect the

presence of aneurysmal lobulation and its relationship to neighboring arteries using shaded surface display (SSD) images [89].

It was found recently that we can use the population mean values instead of the patient-specific material parameters to study the rupture potential of aneurysm [68]. Although the conclusion was based on abdominal aortic aneurysms, it would be a logical extension to apply it to intracranial aneurysms. This implies that it would be possible to study and evaluate the rupture potential of intracranial aneurysms with daughter aneurysms using computer simulation.

## REFERENCE

1. Abruzzo T, Shengelaia GG, Dawson III RC, DS Owens, Cawley CM, Gravanis MB: Histologic and morphologic comparison of experimental aneurysms with human intracranial aneurysms. *AJNR* 19:1309-1314, 1998.
2. Akyuz M, Cetin A, Boztug N, Kazan S, Tuncer R: Effects of the temporary clipping in aneurysm surgery on the remnant. *Acta Neurochir (Wien)* 144:129-136, 2002.
3. Allcock JM, Canham PB: Angiographic study of the growth of intracranial aneurysms. *J Neurosurgery* 45:617-621, 1976.
4. Asari S, Ohmoto T: Natural history and risk factors of unruptured cerebral aneurysms. *Clinical Neurology and Neurosurgery* 95:205-214, 1993.
5. Atlas SW, Sheppard L, Goldberg HI, Hurst RW, Listerud J, Flamm E: Intracranial aneurysms: detection and characterization with MR angiography with use of an advanced postprocessing technique in a blinded-reader study. *Radiology* 203:807-14, 1997.
6. Austin GM: Biomathematical model of aneurysm of the Circle of Willis, the Duffing equation and some approximate solutions. *Math Biosci* 11:163-172, 1971.

7. Austin GM: Equation for model intracranial aneurysm with consideration of small dissipation term. *Math Biosci* 22:277-291, 1974.
8. Austin GM, Schievink W, Williams R: Controlled pressure-volume factors in the enlargement of intracranial aneurysms. *Neurosurgery* 24:722-730, 1989.
9. Bederson JB: Hemodynamics and pathophysiology of giant intracranial aneurysms, in Giant Intracranial Aneurysms (Awad IA, Barrow DL), American Association of Neurological Surgeons, 1995.
10. Bruno G, Todor R, Lewis I, Chyatte D: Vascular remodeling in cerebral aneurysms. *J Neurosurg* 89(3):431-440, 1998.
11. Burleson AC, Strother CM, Turitto VT: Computer modeling of intracranial saccular and lateral aneurysms for the study of their hemodynamics. *Neurosurgery* 37:774-784, 1995.
12. Burleson AC, Turitto VT: Identification of quantifiable hemodynamic factors in the assessment of cerebral aneurysm behavior. *Thrombosis and Haemostasis* 76 (1):118-123, 1996.
13. Canham PB, Ferguson GG: A mathematical model for the mechanics of saccular aneurysms. *Neurosurgery* 17:291-295, 1985.
14. Chitanvis SM, Dewey M, Hademenos G, Powers, WJ, Massoud TF: A nonlinear quasi-static model of intracranial aneurysms. *Neurological Research* 19:489-496, 1997.
15. Crawford T: Some observations on the pathogenesis and natural history of intracranial aneurysms. *J Neurol Neurosurg Psychiatry* 22:259-266, 1959.

16. Crompton M: Mechanism of growth and rupture in cerebral berry aneurysms. *Br Med J* 1:1138-1142, 1966.
17. Danturthi RS, Partridge LD, Turitto VT: Hemodynamics of intracranial lateral aneurysms: Flow simulation studies. *IEEE*: 224-227, 1997.
18. Dickey P, Kailasnath P: The diameter-cube hypothesis: a new biophysical model of aneurysm rupture. *Surg Neurol* 58:166-180, 2002.
19. Drake CG: Ruptured intracranial aneurysms. *Proc. Roy. Soc. Med.* 64:477-481, 1971.
20. DuBoulay GH: Some observations on the natural history of intracranial aneurysms. *Br J Radiol* 38: 721-757, 1965.
21. DuBoulay GH: The natural history of intracranial aneurysms. *American Heart Journal* 73(6):723-729, 1967.
22. DuBoulay GH: The significance of loculation of intracranial aneurysms. *Bull Schweiz Akad Med Wiss* 24(5):480-485, July 1969.
23. Dumont AS, Lanzino G, Kassell NF: Unruptured aneurysms [editorial]. *J Neurosurg* 96:52-56, 2002.
24. Dym CL, Ivey ES: Principles of mathematical modeling. Academic Press, 1980.
25. Early CB, Fink LH: Some fundamental applications of the Law of Laplace in neurosurgery. *Surg Neurol* 6:185-189, 1976.
26. Ferguson GG: Turbulence in human intracranial saccular aneurysms. *J Neurosurg* 33:485-497, 1970.
27. Ferguson GG: Physical factors in the initiation, growth, and rupture of human intracranial saccular aneurysms. *J Neurosurg* 37:666-677, 1972.

28. Ferguson GG, Peerless SJ, Drake CG: Natural history of intracranial aneurysms. *N Eng J Med* 305:99, 1981 (letter).
29. Foutarakis GN, Yonas H, Sclabassi RJ: Saccular aneurysm formation in curved and bifurcating arteries. *AJNR* 20: 1309-1317, August 1999.
30. Frerichs KU, Stieg PE, Friedlander RM: Prediction of aneurysm rupture site by an angiographically identified bleb at the aneurysm neck. *J Neurosurg* 93:517, 2000.
31. Gold HJ: Mathematical modeling of biological systems – an introductory guidebook. John Wiley & Sons, Inc., 1977.
32. Gonzalez CF, Cho YI, Ortega HV, Moret J: Intracranial Aneurysms: Flow analysis of their origin and progression. *AJNR* 13:181-188, 1992.
33. Hademenos GJ: The physics of cerebral aneurysms. *Physics Today* 48:24-30, February 1995.
34. Hademenos GJ, Massoud TF: The physics of cerebrovascular diseases. Springer-Verlag New York, Inc., 1998.
35. Hademenos GJ, Massoud TF: Biophysical mechanisms of stroke. *Stroke*, Vol. 28 (10):2067-2077, 1997.
36. Hademenos GJ, Massoud TF, Turjman F, Sayre JW: Anatomical and morphological factors correlating with rupture of intracranial aneurysms in patients referred for endovascular treatment. *Neuroradiology* 40:755-760, 1998.
37. Hademenos GJ, Massoud T, Valentino DJ, Duckwiler G, Vinuela F: A nonlinear mathematical model for the development and rupture of intracranial saccular aneurysms. *Neurol Res* 16:376-384, Dec 1994.

38. Hademenos GJ, Massoud T, Valentino DJ, Duckwiler G, Vinuela F: A nonlinear mathematical model for the development and rupture of intracranial fusiform aneurysms. *Neurol Res* 16(6):433-438, Dec 1994.
39. Hashimoto T: Dynamic measurement of pressure and flow velocities in glass and silastic model berry aneurysms. *Neurol Res* 6:22-28, 1984.
40. Hassler: Scanning electron microscopy of saccular intracranial aneurysms. *Am J Pathol* 68:511-520, 1972.
41. Hayashi T, Satoh S, Shirane R: Saccular aneurysm-like bleb formation after rupture of the internal carotid-posterior communicating artery aneurysm: a case with interesting angiographic findings. *No Shinkei Geka* 25(1):85-88, 1997.
42. Hinshaw DB, Simmons CR, Leech W, Minckler J, Austin G: Loculated intracranial aneurysms: angiography and possible etiology. *Radiology* 113:101-106, October 1974.
43. <http://hyperphysics.phy-astr.gsu.edu/hbase/ptens.html>
44. Hung EJ, Botwin MR: Mechanics of rupture of cerebral saccular aneurysms. *Journal of Biomechanics* 8:385-392, 1975.
45. The International Study of Unruptured Intracranial Aneurysms Investigators: Unruptured intracranial aneurysms – risk of rupture and risks of surgical intervention. *N Eng J Med* 339:1725-1733, 1998.
46. Jain KK: Mechanism of rupture of intracranial saccular aneurysms. *Surgery* 54:347-350, 1963.

47. Juvela S, Porras, Poussa K: Natural history of unruptured intracranial aneurysms: probability of and risk factors for aneurysm rupture. *J Neurosurg* 93:379-387, 2000.
48. Juvela S: Natural history of unruptured intracranial aneurysms: risks for aneurysm formation, growth, and rupture. *Acta Neurochir [Suppl]* 82:S27-S30, 2002.
49. Kassell NF, Torner JC: Size of intracranial aneurysms. *Neurosurgery* 12:291-297, 1983.
50. Kim C, Kikuchi H, Hashimoto N, Hazama F: Angiographic study of induced cerebral aneurysms in primates. *Neurosurgery* 27:715-720, 1990.
51. Krex D, Schackert, Schackert G: Genesis of cerebral aneurysms – an update. *Acta Neurochir (Wien)* 143:429-449, 2001.
52. Kondo S, Hashimoto N, Kikuchi H, *et al*: Cerebral aneurysms arising at nonbranching sites: an experimental study. *Stroke* 28:398-404, 1997.
53. Lieber BB, Aenis M, Zhao Y, Wakhloo AK: Flow characteristics in a stented and non-stented side wall aneurysm model. *ASME Advances in Bioengineering, BED* 31:379-380, 1995.
54. Low M, Perktold K, Raunig R: Hemodynamics in rigid and distensible saccular aneurysms: a numerical study of pulsatile flow characteristics. *Biorheology* 30:287-298, 1993.
55. MacDonald DJ, Finlay HM, Canham PB: Directional wall strength in saccular brain aneurysms from polarized light microscopy. *Annals of Biomedical Engineering* 28:533-542, 2000.

56. McCormick WF, Acosta-Rua GJ: The size of intracranial saccular aneurysms. *J Neurosurg* 33:422-427, 1970.
57. Massoud TF, Hademenos GJ, Young WL, Gao E, Pile-Spellman J, Vinuela F: Principles and philosophy of modeling in biomedical research. *FASEB J* 12:275-285, 1998.
58. Mizoi K, Yoshimoto T, Nagamine Y: Types of unruptured cerebral aneurysms reviewed from operation video-recordings. *Acta Neurochir (Wien)* 138:965-969, 1996.
59. Mulay A, Feng Y, Meng H, Bendok BR, Guterman LR, Taulbee DB, Hopkins LN. A computational fluid dynamics study on wall shear stress of sidewall aneurysms of varying size and dome-to-neck ratio. 2<sup>nd</sup> joint meeting of EMBS-BMES, Houston, Texas, October 23-26, 2002.
60. Murata T, Tsuruno T, Shimotake K, Terakawa Y, Nishio A, Nishijima Y, Agou I: Management strategies for unruptured cerebral aneurysms. *No Shinkei Geka* 29(10):943-949, 2001.
61. Murthy DNP, Page NW, Rodin EY: Mathematical modeling: A tool for problem solving in engineering, physical, biological and social sciences. Pergamon Press, 1990.
62. Nakase H, Aketa S, Sakaki T, Nakamura M, Aoyama N: Detection of a newly-developed thin-walled out pouching (“bleb”) in an unruptured intracranial aneurysm by computed tomographic angiography. *Acta Neurochir (Wien)* 140:517-518, 1998.

63. Nieto JJ, Torres A: A nonlinear biomathematical model for the study of intracranial aneurysms. *Journal of the Neurological Sciences* 177:18-23, 2000.
64. Nystrom SHM: On factors related to growth and rupture of intracranial aneurysms. *Acta Neuropath. (Berl.)* 16:64-72, 1970.
65. Orz YI, Hongo K, Tanaka Y, Nagashima H, Osawa M, Kyoshima K, Kobayashi S: Risks of surgery for patients with unruptured intracranial aneurysms. *Surg Neurol* 53:21-29, 2000.
66. Parlea L, Fahrig R, Holdsworth DW, Lownie SP: An analysis of the geometry of saccular intracranial aneurysms. *American Journal of Neuroradiology* 20:1079-1089, 1999.
67. Phan TG, Huston J, Brown RD, Wiebers DO, Piepgras DG: Intracranial saccular aneurysm enlargement determined using serial magnetic resonance angiography. *J Neurosurg* 97:1023-1028, 2002.
68. Raghavan ML, Vorp DA: Toward a biomechanical tool to evaluate rupture potential of abdominal aortic aneurysm: identification of a finite strain constitution model and evaluation of its applicability. *Journal of Biomechanics* 33, 475-482, 2000.
69. Sakamoto T, Kwak R, Mizoi K, Ohi T, Katakura R, Suzuki J: Angiographical study of ruptured aneurysm in the multiple aneurysm patients. *No Shinkei Geka. Neurological Surgery* 6(6):549-553, 1978.
70. Sampei T, Mizuno M, Nakajima S, Suzuki A, Hadeishi H, Ishikawa T, Yasui N: Clinical study of growing up aneurysms: report of 25 cases. *No Shinkei Geka* 19:825-830, 1991.

71. San Millan Ruiz D, Tokunaga K, Dehdashti AR, Sugi K, Delavelle J, Rufenacht DA: Is the rupture of cerebral berry aneurysms influenced by the perianeurysmal environment? *Acta Neurochir [suppl]* 82:S31-S34, 2002
72. Sarwar M., Batnitzky S., Schechter M., Liebeskind A., and Zimmer A. E.: Growing intracranial aneurysms. *Radiology* 120:603-607, 1976.
73. Scanarini M, Mingrino S, Giordano R, Baroni A: Histological and ultrastructural study of intracranial saccular aneurysmal wall. *Acta Neurochirurgica* 43:171-182, 1978.
74. Schievink WI: Medical Progress: Intracranial Aneurysms. *The New England Journal of Medicine*, 28-40, January 2, 1997.
75. Schievink WI, Piepgras DG, Wirth FP: Rupture of previously documented small asymptomatic saccular intracranial aneurysms. *J Neurosurg* 76:1019-1024, 1992.
76. Scott S, Ferguson GG, Roach MR: Comparison of the elastic properties of human intracranial arteries and aneurysms. *Can J Physiol Pharmacol* 50:328-332, 1971.
77. Sekhar LN, Heros RC: Origin, growth, and rupture of saccular aneurysms: a review. *Neurosurgery* 8:248-260, 1981.
78. Sekhar LN, Sclabassi RJ, Sun M, Blue HB, Wasserman JF: Intra-aneurysmal pressure measurements in experimental saccular aneurysms in dogs. *Stroke* 19:352-356, 1988.
79. Sorimachi T, Takeuchi S, Koike T, Minakawa T, Tanaka R: Intra-aneurysmal pressure changes during angiography in coil embolization. *Surg Neurol* 48:451-457, 1997.

80. Sprecher W, Wenz W, Haffner HT: Rupture of an intracranial aneurysm – unusual complication of an electric shock. *Forensic Science International* 122:85-88, 2001.
81. Stehbens WE: Etiology of intracranial berry aneurysms. *J Neurosurg*, 70:823-831, 1989.
82. Stehbens WE: Histopathology of cerebral aneurysms. *Arch Neurol* 8:272-285, 1963.
83. Stehbens WE: Hemodynamics and the blood vessel wall. Charles C Thomas, pp. 476-496, 1979.
84. Stehbens WE: Pathology and pathogenesis of intracranial berry aneurysms. *Neurol Res* 12:29-34, 1990.
85. Steiger HJ: Pathophysiology of development and rupture of cerebral aneurysms. *Acta Neurochir Suppl (Wien)* 48:1-57, 1990.
86. Steiger HJ, Poll A, Liepsch DW, Reulen HJ: Basic flow structure in saccular aneurysms: a flow visualization study. *Heart Vessels*, 3:55-65, 1987.
87. Steinberg GK, Chung M: Morphology and structural pathology, in Giant Intracranial Aneurysms (Awad IA, Barrow DL), American Association of Neurological Surgeons, 1995, pp. 1-11.
88. Strother CM, Graves VB, Rappe A: Aneurysm hemodynamics: An experimental study. *AJNR* 13:1089-1095, 1992.
89. Sugahara T, Korogi Y, Nakashima K, Hamatake S, Honda S, Takahashi M: Comparison of 2D and 3D digital subtraction angiography in evaluation of intracranial aneurysms. *AJNR Am J Neuroradiol* 23:1545-1552, 2002.

90. Suzuki J, Ohara H: Clinicopathological study of cerebral aneurysms. Origin, rupture, repair, and growth. *J Neurosurg* 48:505-514, 1978.
91. Tateshima S, Murayama Y, Villablanca JP, Morino T, Takahashi H, Yamauchi T, Tanishita K, Vinuela F: Intraaneurysmal flow dynamics study featuring an acrylic aneurysm model manufactured using a computerized tomography angiogram as a mold. *J Neurosurg* 95:1020-1027, 2001.
92. Tateshima S, Murayama Y, Villablanca JP, Morino T, Nomura K, Tanishita K, Vinuela F: In vitro measurement of fluid-induced wall shear stress in unruptured cerebral aneurysms harboring blebs. *Stroke* , 2002
93. Toth M, Nadasy GL, Nyary I, Kerényi T, Orosz M, Molnarka G, Monos E: Sterically inhomogenous viscoelastic behavior of human saccular cerebral aneurysms. *J Vasc Res* 35:345-355, 1998.
94. Toth M, Nadasy GL, Nyary I, Kerényi T, Orosz M, Monos E: Do human intracranial aneurysms have inhomogeneous viscoelastic properties? *Pathophysiology* 5 (SUPPL 1 JUN): 249-EOA, 1998.
95. Tsuchiya K, Katase S, Yoshino A, Hachiya J, Yodo K: Preliminary evaluation of volume-rendered three-dimensional display of time-of-flight MR angiography in the diagnosis of intracranial aneurysms. *Neuroradiology* 43(8):633-636.
96. Tsutsumi K, Ueki K, Morita A, Kirino T: Risk of rupture from incidental cerebral aneurysms. *J Neurosurg* 93:550-553, 2000.
97. Ujiie H, Tachibana H, Hiramatsu O, Hazel AL, Matsumoto T, Ogasawara Y, Nakajima H, Hori T, Takakura K, Kajiyama F: Effects of size and shape (aspect

- ratio) on the hemodynamics of saccular aneurysm: a possible index for surgical treatment of intracranial aneurysms. *Neurosurgery* 45:119-130, 1999.
98. Ujiie H, Tamano Y, Sasaki K, Hori T: Is the aspect ratio a reliable index for predicting rupture of a saccular aneurysm? *Neurosurgery* 48:495-503, 2001.
99. Vega C, Kwoon JV, Lavine SD: Intracranial aneurysms: current evidence and clinical practice. *Am Fam Physician* 66:601-608, 2002.
100. Weir B: Intracranial aneurysms and subarachnoid hemorrhage: An overview, in Wilkins R, Rengachary SS (eds): *Neurosurgery*. New York, McGraw-Hill, 1985, Vol. 2.
101. Weir B: Unruptured intracranial aneurysms: a review. *J Neurosurg* 96:3-42, 2002.
102. Weir B, Disney L, Karrison T: Sizes of ruptured and unruptured aneurysms in relation to their sites and the ages of patients. *J Neurosurg* 96:64-70, 2002.
103. Wiebers DO, Whisnant JP, Sundt TM, O'Fallon WM: The significance of unruptured intracranial saccular aneurysms. *J Neurosurg* 66:23-29, 1987.
104. Yamamoto Y, Yamaguchi T: Computational fluid mechanical simulation of the spontaneous deformation and alignment of the endothelial cell model under fluid shear stress. *ASME Advances in Bioengineering, BED* 33:85-86, 1996.
105. Yates FE: Good manners in good modeling: Mathematical models and computer simulations of physiological systems. *Am J Physiol* 234:R159-R160, 1978.
106. Young B, Meacham WF, Allen JH: Documented enlargement and rupture of a small arterial sacculation. *J Neurosurg* 34:814-817, 1971.

# APPENDICES

## Appendix A: Source code

All the scripts are written in MATLAB<sup>®</sup> 6.1.

### A.1. “*draw\_aneurysm.m*”

This Matlab<sup>®</sup> function draws the geometry of an aneurysm with a daughter aneurysm at the dome.

```
function draw_aneurysm(mu, lambda,h)

%draw_aneurysm(mu, lambda,h)
%This program draws a daughter aneurysm model with orifice index mu and aspect ratio
lambda;
%h is the thickness of the lines.

x1=linspace(-1,-mu,50000);
x2=linspace(mu,1,50000);
x3=linspace(-1,-0.95,50000);
x4=linspace(0.95,1,50000);
y1 = sqrt(1 - x1.^2);
y2 = sqrt(1 - x2.^2);
y3 = -sqrt(1 - x3.^2);
y4 = -sqrt(1 - x4.^2);
```

```

a1 = mu;
h1 = mu*lambda;
r = (h1^2 + a1^2)/(2*h1);
y0 = h1 + sqrt(1-mu*mu) - r;

x=linspace(-mu,mu,50000);
y = y0 + sqrt(r*r - x.*x);

plot(x1,y1,x2,y2, x3,y3, x4,y4, x,y);
set(findobj('Type','line'),'Color','k','LineWidth',h);
axis equal;

x1 = linspace(-r,-mu,50000);
x2 = linspace(mu,r,50000);
y1 = y0 - sqrt(r*r - x1.*x1);
y12 = y0 + sqrt(r*r - x1.*x1);
y2 = y0 - sqrt(r*r - x2.*x2);
y22 = y0 + sqrt(r*r - x2.*x2);

if lambda>1 % If the daughter aneurysm is past a hemisphere
    hold on;
    plot(x1,y1, x1,y12, x2,y2, x2,y22);
    set(findobj('Type','line'),'Color','k','LineWidth',h);
end

axis([-1.03 1.03 -0.35 1.5]);
axis off;

return;

```

## A.2. “*eta\_lambda.m*”

This Matlab<sup>®</sup> function plots the curve of the relative tensile stress  $\eta$  as a function of the aspect ratio  $\lambda$  at the orifice index  $\mu = 0.1, 0.3$  and  $0.5$  (Figure 5.1).

```

function eta_lambda()

%lambda_eta_meng_1205()

```

```

%This program draws the curve of the relative tensile stress as a function of the aspect
ratio lambda.
% mu = a'/R is the orifice index
% lambda =h'/a' is the aspect ratio

mu=0.1;
lambda_i = 1/mu - sqrt(1/mu/mu-1);
lambda = linspace (lambda_i,2.48,1000);

coef = mu*(1+sqrt(1-mu*mu))/4;
eta = coef*(1+lambda.*lambda).^2./lambda;

plot(lambda,eta);
hold on;

%-----
mu=0.3;
lambda_i = 1/mu - sqrt(1/mu/mu-1);
lambda = linspace (lambda_i,1.49,1000);
lambda2 = linspace (1.5, 2,1000);

coef = mu*(1+sqrt(1-mu*mu))/4;

eta = coef*(1+lambda.*lambda).^2./lambda;
eta2 = coef*(1+lambda2.*lambda2).^2./lambda2;

plot(lambda,eta,lambda2,eta2,'k--');
hold on;

%-----
mu=0.5;
lambda_i = 1/mu - sqrt(1/mu/mu-1);
lambda = linspace (lambda_i,1.09,1000);
lambda2 = linspace (1.1, 2,1000);

coef = mu*(1+sqrt(1-mu*mu))/4;
eta = coef*(1+lambda.*lambda).^2./lambda;
eta2 = coef*(1+lambda2.*lambda2).^2./lambda2;

plot(lambda,eta,lambda2,eta2,'k--');
hold on;

```

```

xlabel('Height/radius ratio (\lambda = h));
ylabel('Relative wall stress (\eta)');
axis([0 2.5 0 1.2]); hold on;
plot([0 2.5],[1 1],'k--'); hold on;
plot(1.07,1,'*', 1.4712, 1, '*',2.454,1, '*')

return;

```

### A.3. “two\_phase\_grow”

This Matlab<sup>®</sup> function plots two-phase growth mode of a daughter aneurysm as described in Section 5.4.

```

function two_phase_grow(mu, end_lambda)

%This function plots the two-phase growth of a daughter aneurysm
%mu = a/R is the orifice index;
%end_lambda is the aspect ratio of the daughter aneurysm when it ruptures.

lambda_i = 1/mu - sqrt(1/mu/mu-1);
lambda_minimal = sqrt(3)/3;
k_slow = 1 - lambda_minimal;
k_fast = 20*k_slow;
t_fast = (lambda_minimal-lambda_i)/k_fast;
t_slow = (end_lambda - lambda_minimal)/k_slow;

t1 = linspace(0,t_fast, 10000);
t2 = linspace(t_fast, t_slow, 10000)
lambda1 = lambda_i + k_fast*t1;
lambda2 = lambda_minimal + k_slow*(t2-t_fast);

coef = mu0*(1+sqrt(1-mu0*mu0))/4;
eta1 = coef*(1+lambda1.*lambda1).^2./lambda1;
eta2 = coef*(1+lambda2.*lambda2).^2./lambda2;

subplot(2,1,1);plot(t1,lambda1,t2,lambda2);
subplot(2,1,2);plot(t1,eta1,t2,eta2);

return;

```